Silicon Photonics

Bahram Jalali, *Fellow, IEEE*, and Sasan Fathpour, *Member, IEEE*

Invited Paper

***Abstract*—After dominating the electronics industry for decades, silicon is on the verge of becoming the material of choice for the photonics industry: the traditional stronghold of III–V semiconductors. Stimulated by a series of recent breakthroughs and propelled by increasing investments by governments and the private sector, silicon photonics is now the most active discipline within the field of integrated optics. This paper provides an overview of the state of the art in silicon photonics and outlines challenges that must be overcome before large-scale commercialization can occur. In particular, for realization of integration with CMOS very large scale integration (VLSI), silicon photonics must be compatible with the economics of silicon manufacturing and must operate within thermal constraints of VLSI chips. The impact of silicon photonics will reach beyond optical communication—its traditionally anticipated application. Silicon has excellent linear and nonlinear optical properties in the midwave infrared (IR) spectrum. These properties, along with silicon's excellent thermal conductivity and optical damage threshold, open up the possibility for a new class of mid-IR photonic devices.**

***Index Terms*—CMOS, continuum generation, erbium-doped silicon, integrated photonics, nonlinear optics, optical amplifier, optical modulator, photodetector, photovoltaic effects, power dissipation, Raman laser, Raman scattering, silicon laser, silicon-on-insulator, silicon photonics, silicon-rich oxide, VLSI, wavelength conversion.**

I. Introduction

THE ROOTS of silicon photonics can be traced back to the pioneering works of Soref and Petermann in the late 1980s and early 1990s [1]–[4]. The early work stimulated activities that resulted in substantial progress, mostly in passive devices, in the 1990s [4]–[11]. The technology boom of the late 1990s and the concomitant abundance of the private capital triggered a rapid growth of the field. While the level of private funding did diminish in the early 2000s, it served as a catalyst by raising awareness to this new technology. This led to increased level of investments by large corporations and government agencies that have fueled spectacular progress in the last five years.

Rather than attempting to provide a comprehensive historical review of silicon photonics, this paper offers a sampling of the most recent developments, combined with the authors' perspective on the promises of this technology and the challenges that remain before the benefits can come to fruition. We begin by describing the motivation for silicon photonics: both the traditional argument that is still valid and the new insight that has recently been gained. This will be followed by applications that are expected to be impacted. Next, this paper discusses recent developments in components ranging from passive devices to modulators, detectors, and light amplifiers and sources. This paper concludes by looking ahead at challenges as well as potentials of the technology that have not been fully recognized in the past.

The traditional argument in favor of silicon photonics is based on its compatibility with the mature silicon IC manufacturing. Silicon wafers have the lowest cost (per unit area) and the highest crystal quality of any semiconductor material. The industry is able to produce microprocessors with hundreds of millions of components, all integrated onto a thumb-size chip, and offer them at such a low price that they appear in consumer electronics. Silicon manufacturing represents the most spectacular convergence of technological sophistication and economics of scale.

Creating low-cost photonics for mass-market applications by exploiting the mighty IC industry has been the traditional motivation for silicon photonics researchers. Another motivation is the availability of high-quality silicon-on-insulator (SOI) wafers, an ideal platform for creating planar waveguide circuits. The strong optical confinement offered by the high index contrast between silicon ($n = 3.45$) and SiO_2 ($n = 1.45$) makes it possible to scale photonic devices to the hundreds of nanometer level. Such lateral and vertical dimensions are required for true compatibility with IC processing. In addition, the high optical intensity arising from the large index contrast (between Si and SiO_2) makes it possible to observe nonlinear optical interactions, such as Raman and Kerr effects, in chip-scale devices. This fortuitous outcome has enabled optical amplification, lasing, and wavelength conversion, functions that until recently were perceived to be beyond the reach of silicon.

The above arguments represent the traditional and still valid motivation in favor of silicon photonics. However, the case for silicon photonics is even stronger. Silicon has excellent material properties that are important in photonic devices. These include high thermal conductivity ($\sim 10\times$ higher than GaAs), high optical damage threshold ($\sim 10\times$ higher than GaAs), and high third-order optical nonlinearities. Kerr effect is 100 times larger, whereas Raman effect is 1000 times stronger than those in silica fiber. Fig. 1 shows the absorption spectrum of silicon, boasting a low-loss wavelength window extending from 1.1 to nearly

Manuscript received June 8, 2006; revised September 27, 2006. This work was supported by the Defense Advanced Research Project Agency (DARPA).

The authors are with the Department of Electrical Engineering, University of California, Los Angeles, CA 90095-1594 USA.

Color versions of Figs. 2–6, 8–10, 13–16, 18, and 19 are available online at http://ieeexplore.ieee.org.

Digital Object Identifier 10.1109/JLT.2006.885782

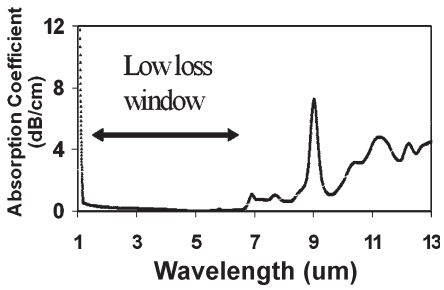

Fig. 1. Absorption spectrum of silicon grown by the Czochralski method and measured using Fourier transform infrared spectroscopy.

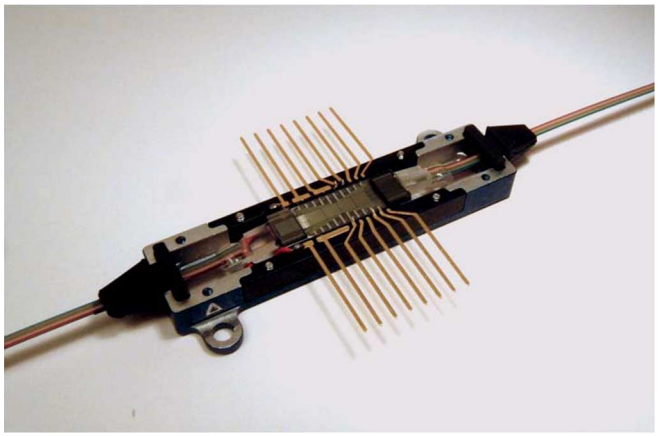

Fig. 2. Eight-channel VOA representing a commercial silicon photonics product [13]. The device is manufactured by Kotura Corporation and is used for automatic channel equalization in add/drop multiplexers in Nortel's metropolitan area network gear (figure courtesy of A. Martin).

7 μm [12]. Far from being limited to the near-infrared (IR) data communication band of 1.3–1.55 μm, silicon is an excellent material in the midwave IR spectrum.

II. Applications

Boasting low-cost substrates and mature manufacturing infrastructure, silicon photonics represents a path toward mass manufacturing of discrete optical components, as well as integrated transceivers for synchronous optical network, gigabit Ethernet, and optical backplane markets. An example of a commercial silicon photonic component is the eight-channel variable optical attenuator (VOA) manufactured by Kotura Corporation [13]. The product, as shown in Fig. 2, is used for automatic channel equalization in add/drop multiplexers and appears in Nortel Corporation's products aimed at metropolitan networks. Fig. 3 describes what might be a next generation of silicon photonic product. The prototype device is a four-channel wavelength-division multiplexing (WDM) transceiver reported by Luxtera Corporation, Carlsbad, CA [14]. It is fabricated on a 90-nm SOI CMOS process and monolithically integrates wavelength filters, photodetectors, electronic amplifiers, and drivers. The only components that are not monolithically integrated are four InP lasers that are flip-chip bonded onto the silicon substrate.

The second mainstream application envisioned for silicon photonics is optical interconnects for CMOS electronics [15]. Fig. 4 highlights the communication bottleneck in very large scale integration (VLSI) electronics. The Cell processor developed jointly by Sony and IBM is at the heart of Sony's Playstation 3 game console. The eight-core processor has an internal computation power of 256 giga floating point operations per second (GFLOPS) and communicates with the peripheral graphics processor and memory at data rates of 25 Gb/s or higher [16], [17]. Such data rates challenge copper-based interconnects.

Conventional wisdom holds that optical interconnects are much better suited than copper interconnects in handling such high data rates. However, with the use of equalization and other signal processing techniques, copper interconnects can address higher and higher data rates, albeit at the cost of higher power dissipation. Therefore, for optical interconnects to replace their copper counterparts, they must provide a lower power solution. Up to now, the power dissipation of silicon photonic devices has rarely been addressed by the research community. However, given critical importance of power dissipation in integrated systems, it is a topic that must take central stage in future work.

In addition to optical interconnects, several other applications are envisioned for silicon photonics. The technology can also play a role in biosensing applications. A disposable mass-produced sensor would be attractive as it could grow the market for biosensors. Sensor applications are somewhat different from optical communication as there are other very low cost optical technologies that compete in this space [18]. One likely application area for silicon photonics is the so-called lab-on-a-chip in which both reaction and analysis are performed in a single device. In the future, this could be extended to include electronic intelligence and wireless communications—key functions that will be needed to create intelligent sensor networks for environmental monitoring.

An example of an advanced biosensor being developed in academia (at Vanderbilt University) is shown in Fig. 5 [19]. The device represents a label-free biosensor that is inspired by the surface plasmon resonance (SPR) sensor, although it uses a different waveguiding and transduction mechanism. The transducer is a porous silicon waveguide into which light is coupled via a prism. The coupling angle depends on the refractive index of the porous silicon, which changes when biomolecules bind to the receptors inside the pores. The sensor is expected to be more sensitive than an SPR due to the enhanced interaction between the electromagnetic field and the biomolecules in nanoscale dimensions of pores [19].

III. Passive Devices

The basic requirement for virtually all integrated optical devices is low propagation losses in waveguides and cavities. Owing to the high index contrast between a silicon waveguide and its surrounding medium (air or SiO_2), surface roughness results in significant scattering losses. Consequently, silicon waveguides are characterized by losses in the range of 0.1–3 dB/cm depending on the dimensions and processing conditions. In general, losses are higher in smaller waveguides where the field intensity at the silicon surface is high. Thermal oxidation can be used to reduce the roughness on the waveguide

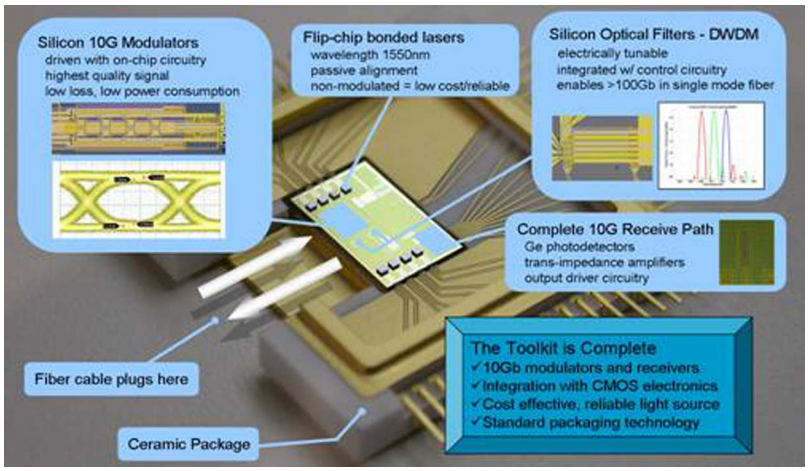

Fig. 3. Prototype 10-Gb/s transceiver from Luxtera Corporation [14]. The four-channel WDM transmitter/receiver is fabricated using a 90-nm SOI CMOS process and monolithically integrates all functionalities, except the InP-based lasers that are flip-chip bonded onto the silicon substrate (figure courtesy of C. Gunn).

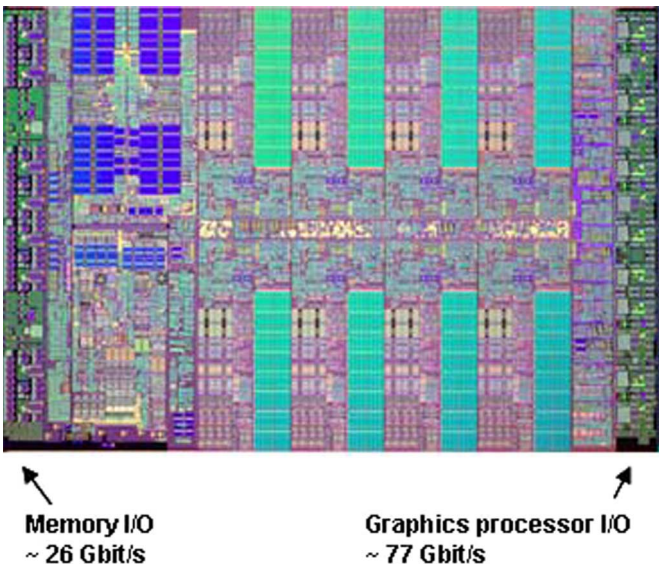

Fig. 4. Cell processor from Sony Corporation is at the heart of the Playstation 3 game console. The eight-core processor has an internal computation power of 256 GFLOPS and communicates with the peripheral graphics processor and memory at speeds of 25 Gb/s or higher [16], [17]. The chip underscores the need for high-speed interconnects for intrachip and interchip communications (figure courtesy of K. Kishima, Sony Corp).

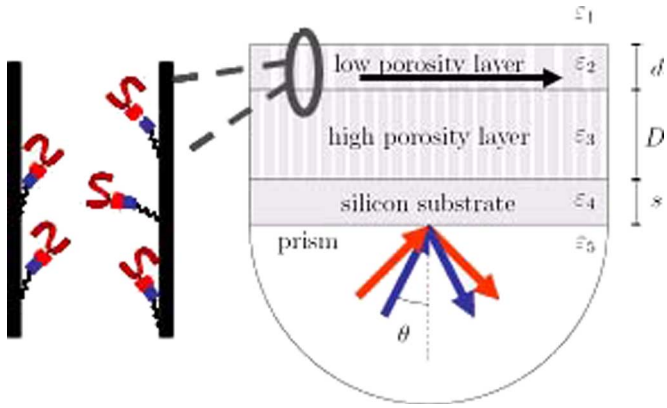

Fig. 5. Silicon photonic biosensor consisting of a porous silicon waveguide into which light is coupled via a prism. The coupling angle depends on the refractive index of the porous silicon, which changes when biomolecules bind to the receptors inside the pores [19] (figure courtesy of S. Weiss).

sidewall, and its effect on the sidewall morphology has been studied extensively (see, for example, [20]). Oxidation drastically reduces the roughness of Si/SiO_2 interface, with the effect being more pronounced with increasing oxidation time and temperature. It has been found that oxidation at higher temperatures ($\sim$1100 °C) is preferred as it offers an extremely smooth sidewall without deformation of waveguide's cross-sectional profile [20].

Compatibility with CMOS technology requires highly efficient use of wafer real estate. The high refractive index of silicon makes it possible to reduce the optical mode size to approximately 0.1 μm^2 [21], [22], i.e., on the same scale as typical dimensions encountered in CMOS VLSI. The high index contrast between silicon and the SiO_2 lower cladding layer makes it possible to create ultracompact waveguide bends, another requirement for creating real-estate efficient devices. Using such silicon wire waveguides, ultrasmall channel-dropping lattice filters have been fabricated [23]. The waveguide's low-loss bends with 2.5-μm radius have reduced the total length of the filter to less than 100 μm and have resulted in a large free spectral range of more than 80 nm for the filters.

Despite the severe modal mismatch between the silicon wire waveguide (effective area, $A_{\text{eff}} \sim 0.1\ \mu m^2$) and a single-mode fiber ($A_{\text{eff}} \sim 50\ \mu m^2$), efficient fiber–waveguide coupling can be achieved using the inverse taper approach [22], [24]–[26]. Resembling the approach used in compound semiconductor lasers, this technique relies on the gradual expansion of a core guided mode into a much larger cladding guided mode. Coupling loss as low as 0.2 dB has been demonstrated from a single-mode fiber to a silicon wire waveguide [24]. Another approach for efficient fiber-to-waveguide coupling is using surface gratings etched onto silicon [14], [27], [28]. A curved grating geometry simultaneously performs phase matching and focusing [28]. The fiber–waveguide coupling losses of 1 dB are

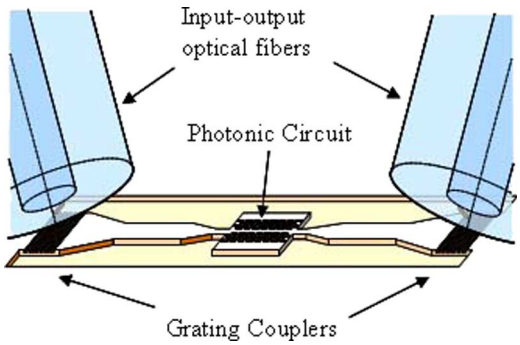

Fig. 6. Efficient fiber to waveguide coupling via surface gratings [27]. The normal-incidence geometry resembles conventional circuit testing and may make it possible to use existing automated test equipment during manufacturing of photonic circuits.

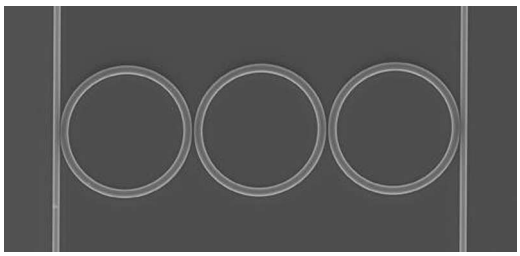

Fig. 7. SiN waveguide add/drop filter with a 50-dB extinction ratio demonstrated at MIT [31] (figure courtesy of E. Ippen).

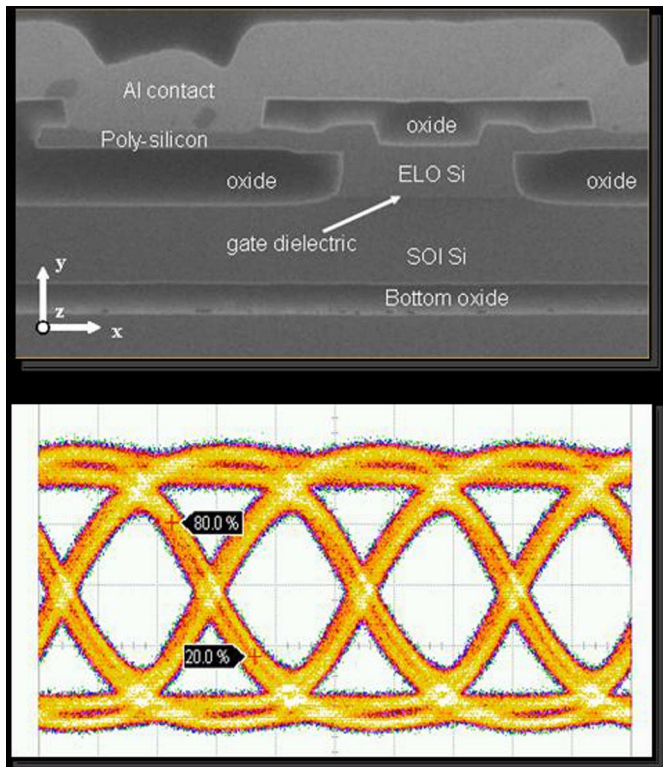

Fig. 8. (Top) Intel's silicon waveguide-based MOS capacitor phase shifter [40]. It comprises a 1.0-μm n-doped crystalline Si (the Si layer of the SOI wafer) on the bottom and a 0.55-μm p-doped crystalline Si on the top with a 10.5-nm gate dielectric—a multilayer stack of silicon dioxide and nitride—sandwiched between them. ELO: epitaxial lateral overgrowth. (Bottom) 10-Gb/s eye diagram for an MZ modulator that uses the MOS phase shifter (figure courtesy of M. Paniccia).

obtained in experiments with a theoretical lower limit of 0.2 dB [28]. The normal-incidence geometry resembles conventional circuit testing (Fig. 6) [27] and may make it possible to use existing automated test equipment during product manufacturing.

One of the important applications of passive devices is the optical filters used for wavelength multiplexing and demultiplexing. Arrayed waveguide grating, the workhorse of WDM communication, was demonstrated using SOI waveguides as early as 1997 [10]. More recently, microring and microdisk structures have been extensively explored for the same applications [22], [29], including devices with microelectromechanical system tunability [30]. A key challenge in such structures is achieving a high extinction ratio, a task that is difficult due to fabrication-induced errors. Recently, an add/drop filter with an impressive 50-dB extinction ratio has been demonstrated by Popovic *et al.* at Massachusetts Institute of Technology (MIT) [31]. The SiN waveguide device, as shown in Fig. 7, achieved this performance without post fabrication trimming and offers flat-top bandpass performance with 2 dB of drop loss.

IV. Modulators

Silicon is not an ideal material for electrooptic modulation. The linear electrooptic effect, the so-called Pockel effect that is the basis of traditional $LiNbO_3$ modulators, is absent in silicon due to its centrosymmetric crystal structure. This leaves the plasma dispersion effect as the only viable mechanism to achieve fast modulation [32]. The plasma dispersion effect is related to the density of free carriers in a semiconductor, which changes both the real and imaginary parts of the refractive index. This widely employed approach can be traced back to the classic work of Soref *et al.* [2], [32]–[35] followed by the early work of Tang *et al.* [36]–[38]. They demonstrated that waveguide switches and modulators can be fashioned in silicon by taking advantage of the linear dependence of refractive index and absorption coefficient on carrier density. The basic mechanism is well understood and is described in excellent review articles about this topic [39]. Here, we highlight some of the recently reported devices that might arguably be considered as the state of the art.

Researchers from Intel Corporation have demonstrated a silicon-based optical modulator that can operate at 10 Gb/s [40]. A schematic of the reported device is shown in Fig. 8 and bears resemblance to a metal–oxide–semiconductor (MOS) capacitor. The structure consists of n-type crystalline silicon with an upper "rib" of p-type silicon created by epitaxial lateral overgrowth (ELO). The n-type and p-type regions are separated by a thin insulating oxide layer. Upon application of a positive voltage to the p-type silicon, charge carriers accumulate at the oxide interface, changing the refractive index distribution in the device. This index change, in turn, induces a phase shift that is converted to intensity modulation in a Mach–Zehnder (MZ) interferometer. The modulator has demonstrated operation at 10 Gb/s (Fig. 8). The advantage of this approach is that the MOS structure lends itself to integration with CMOS. The

device achieves a 3.8-dB modulation depth at a voltage of 1.4 V and has an electrooptic modulation metric of 3.3 V · cm. This is a figure-of-merit representing the voltage required to perform on–off switching of light in a 1-cm-long waveguide phase shifter. The total loss was 19 dB, corresponding to 10 dB/cm of waveguide propagation loss and 9 dB of coupling loss. Luxtera Inc., which is a start-up company, has also announced a 10-Gb/s silicon carrier-depletion modulator [14]. The device exhibits 5 dB of modulation depth with 2.5 V of voltage swing with a waveguide propagation loss of 1–3 dB/cm. It uses grating couplers with a loss of 3 dB for the pair of couplers. As a benchmark, commercial $LiNbO_3$ optical modulators exhibit 2.5 dB of total fiber-to-fiber loss (fiber coupling plus waveguide propagation losses) with a switching voltage of about 4 V (for $\sim$20-dB modulation depth) and a bandwidth of 20 Gb/s [41]. Therefore, while impressive progress has been made in silicon devices in a relatively short time, further improvements are still necessary in silicon to challenge $LiNbO_3$ modulators in performance. Fortunately (for silicon), $LiNbO_3$ modulators are too expensive to qualify for use in local area networks and backplane applications, tilting the balance in favor of silicon.

The weak electrooptic effect in silicon requires long devices and hinders high integration levels, thus increasing the cost. Cavity enhancement can, in principle, lead to efficient modulation [42]–[45], although the resulting narrow-band spectrum will require wavelength control of lasers with a concomitant increase in cost. The microcavity facilitates confinement of the optical field in a small region, and the transmission of the device near its resonance is highly sensitive to small index changes in the cavity. A compact device using a ring resonator (10 μm diameter) has recently been demonstrated by Lipson *et al.* at Cornell University [44], [45]. The highly scaled devices used waveguides 450 nm in width and 250 nm in height. Free carriers can be introduced optically via two-photon absorption (TPA) using ultrashort pulses and electrically via carrier injection. The enhancement of the power in the resonant structure reduces the power requirement for switching. Modulation depths up to 15 dB were measured with less than 0.3-V bias voltage change in the electrical version [45].

Free-carrier modulation of Raman gain has been proposed and demonstrated as a means to achieve optical modulation [46]. A Raman laser was combined with a p-i-n silicon modulator, which was used to inject free carriers to suppress lasing in the device and hence introduce modulation. A relatively large separation of the p and n regions of 8 μm was used to perform the function, resulting in a low modulation bandwidth in the megahertz range [46].

V. Detectors

Photodetectors are perhaps the oldest and best understood silicon photonic devices. Commercial products operate at wavelengths below 1000 nm, where band-to-band absorption occurs. Additionally, used in conjunction with scintillators, they are widely used as X-ray detectors that are used in medical computed tomography equipment and airport luggage scanners.

For application in fiber-optic communication, silicon is not the right material since it is transparent in the 1300- and 1550-nm operating wavelengths of these networks [47]. With its smaller bandgap, germanium has strong absorption at these wavelengths—a motivation for the early work on photodetectors with an active layer made of GeSi [48]–[50] as well as SiGeC alloys [51].

The lattice constant of Ge is 4% larger than that of Si. The strain resulting from lattice mismatch modifies the band structure and causes dislocation defects that increase the leakage current of the p-i-n photodetector. Ge does not form a stable oxide, and the lack of a high-quality passivation layer for Ge also makes it difficult to achieve a low dark current. Interestingly, by scaling the device to smaller dimensions, a higher dark current can be tolerated. For a given dark current density (in amperes per square centimeter), the dark current decreases with detector area. Hence, to the extent that the signal can be coupled into the smaller device, a given signal-to-noise ratio can be achieved with a higher dark current density.

Strain limits the thickness of Ge layers that can be epitaxially grown on silicon. A thin Ge layer is preferred from the bandwidth point of view as it minimizes the carrier transit time, but it comes at the expense of reduced absorption and diminished responsivity. A waveguide p-i-n geometry is preferred over a normal-incidence design since it allows independent optimization of absorption volume and transit time.

With solid understanding of material and device-related issues, excellent progress is being made toward Ge on silicon detectors [52] that are approaching III–V detectors in performance [53]–[57]. TPA can be used for low-speed detection of below-bandgap radiation. Such detectors have been used as autocorrelators [58], [59] and as phase detectors for clock recovery using an optical phase-locked loop [60]. Using helium implantation as a means of enhancing the absorption (photoresponse) of Si below the bandgap, photodetection in 1440–1590 nm has been recently proposed and demonstrated for power-monitoring purposes [61].

VI. Optical Amplifiers and Lasers

The creation of silicon optical amplifiers and lasers has often been considered as the holy grail of silicon photonics because of its potential payoff as well as the significant challenge posed by nature. Silicon has an indirect band structure, which means that conduction and valence bands do not occur at the same value of crystal momentum. Because visible or IR photons have negligible momentum (compared to that of the electron), the deexcitation of an electron (recombination) needs to be mediated by emitting or absorbing a phonon to conserve momentum. Such second-order radiative recombination events do not occur frequently, as characterized by a very long lifetime that is in the order of 1 s. The experimentally measured lifetime in silicon is in the millisecond to microsecond range, depending on the impurity or defect concentration. This suggests that the desired radiative processes are insignificant compared to undesired nonradiative recombination. Even when using silicon with the highest purity, devices have an electrical-to-optical conversion efficiency of only $10^{-4}-10^{-3}$. The situation would be different if one could break free of the low radiative recombination rate of bulk silicon.

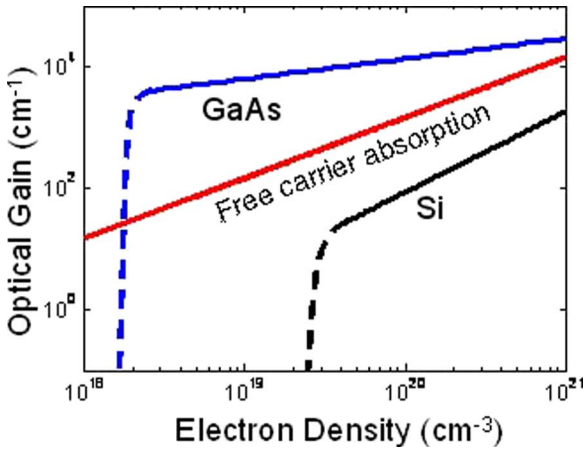

Fig. 9. Optical gain for Si and GaAs showing that FCA results in net loss in Si but not in GaAs [63]. In practice, Auger recombination becomes significant at carrier densities of 10^{19} cm^{-3} and higher in silicon, with a lifetime that decreases quadratically with carrier density.

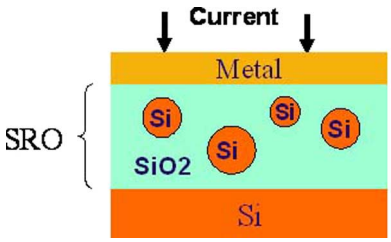

Fig. 10. SRO embedded in MOS structure used for electrical pumping. The conduction mechanism is electron tunneling through the SiO_2. By increasing the conductivity of the SiO_2, silicon nanoparticles reduce the required voltage and hence reduce device degradation and failure over time.

A. Optical Gain in Bulk Silicon

Fig. 9 shows the optical gain in Si and GaAs as a function of injected carrier density [62]. Unfortunately, when carriers are injected, there is optical absorption present due to intraband transitions of carriers. The free-carrier absorption (FCA) is described by Drude's model and depends linearly on the electron–hole pair density $(\sim N)$. The numerical constant of proportionality is roughly the same for GaAs and Si. At a wavelength of 1550 nm, the loss per unit length computes to

$$\alpha_{\mathrm{FCA}} = 1.45 \times 10^{-17} \times N\ (\mathrm{cm}^{-3}) \quad (\mathrm{in\ cm}^{-1}).$$

We see in Fig. 10 that for GaAs, the high rate of direct transitions easily overwhelms the FCA loss, resulting in significant net optical gain. In silicon, however, the low rate of indirect radiative recombination, while constituting a finite gain, is insufficient to overcome the FCA. Consequently, bulk silicon exhibits a net optical loss. We note that the carrier density at which gain appears depends on the effective density of states in the bands, a quantity that is much lower for GaAs than Si. This difference also favors GaAs. Auger recombination becomes significant at carrier densities approaching 10^{19} cm^{-3}, with a lifetime that decreases as N^{-2}. Hence, achieving carrier densities of 10^{19} cm^{-3} and beyond will not be practical as it will require excessively large current densities. The lesson we draw from the above results is that FCA plays the pivotal role in optical amplification and hence lasing in silicon. In any attempt to create a silicon laser, one is well advised not to lose sight of this detrimental yet central phenomenon.

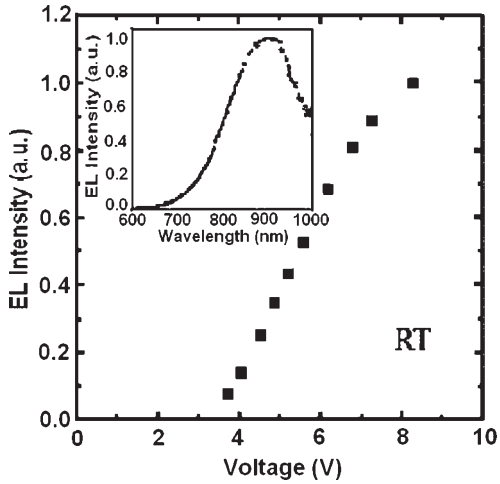

Fig. 11. Electroluminescence of SRO pumped with a MOS junction [64].

While there have been numerous approaches aimed at overcoming or circumventing this limitation, most belong to one of three main categories: 1) overcoming the indirect band structure by using spatial confinement of the electron, 2) introducing rare-earth impurities as optically active dopants, and 3) using Raman scattering to achieve optical gain. Below, we briefly review the salient features of each approach, with the understanding that the length limitation of this paper prevents us from citing most contributions to the field. A more comprehensive review can be found in [63].

B. Quantum Confinement and Erbium Doping

According to the Heisenberg uncertainty principle, when an electron is localized, its momentum becomes uncertain. This phenomenon may offer a solution to the indirect bandgap of silicon. An interesting case study is GaP, the semiconductor that is used for light-emitting devices despite its indirect bandgap. The device works because momentum conservation requirement is relaxed when an electron is localized at a nitrogen impurity site.

In silicon, a popular approach to quantum confinement has been the use of silicon nanocrystals that occur naturally in a silicon-rich oxide (SRO) thin film. When a SiO_x $(x < 2)$ film is subjected to high-temperature annealing, the excess silicon leaves the oxide matrix and forms nanometer-size grains of crystalline silicon dispersed throughout the oxide (Fig. 10). The nanocrystals are excited by pumping the material with a high-intensity light beam. Electrical pumping has also been demonstrated by creating a MOS structure shown in Fig. 10. Electroluminescence is observed in these structures with unipolar (Fig. 11) [64] and bipolar injections [65]. Several research groups, notably at the University of Trento, Trento, Italy, and the University of Rochester, Rochester, NY, have reported optically pumped gain in these films [66], [67]. However, the observed characteristics cannot be explained on the basis of

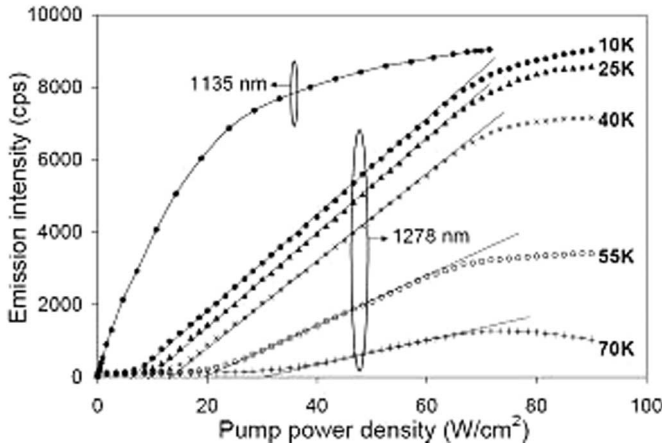

Fig. 12. Optical input–output characteristics of SOI film patterned with a 2-D periodic array of holes. A threshold behavior is observed for emission at a wavelength of 1278 nm. Attributed to lasing, the behavior occurs at temperatures below 70 K. No such behavior was observed at the secondary emission wavelength of 1135 nm that originates from the substrate [70].

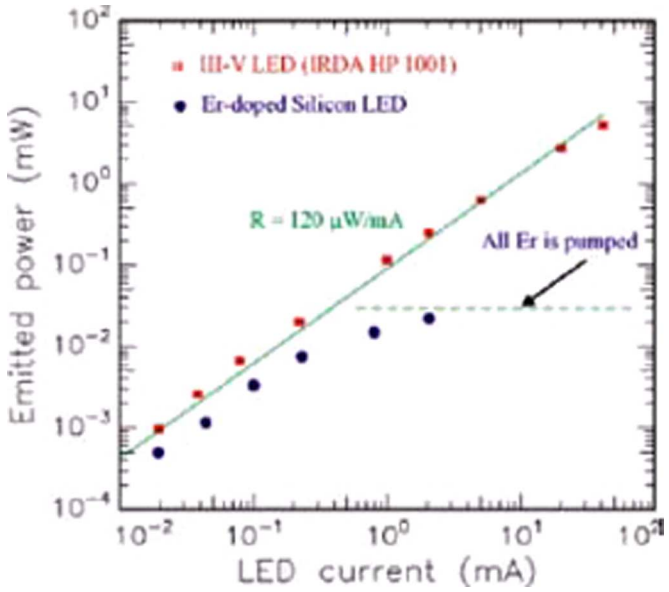

Fig. 13. Light-current characteristics of erbium-doped SRO diode. The diode exhibits high efficiency comparable to a GaAs LED. However, the output saturates at a much lower value of tens of microwatts [72].

electron localization in the nanocrystals, and the observations are highly dependent on how the sample was prepared, with some showing gain and others exhibiting pump-induced loss. Consequently, questions remain regarding the nature of the observed optical gain and the reproducibility of the results [68], [69]. Additionally, the emission wavelength is in the 800- to 900-nm range, i.e., outside of the two standard telecommunication bands centered at 1320 and 1550 nm. This approach is discussed in depth in recent review articles by Fauchet [68] and Pavesi [69].

Other attempts at exploiting quantum confinement in defect sites or in intentionally formed quantum structures show promise. Researchers at Brown University, Providence, RI, have reported evidence of lasing at cryogenic temperatures [70]. A two-dimensional (2-D) array of nanometer size holes was etched into a thin film of silicon that resides on oxide layer. The sample was cleaved (forming mirrors) and pumped optically. As shown in Fig. 12, the optical input–output characteristics show a threshold behavior for emission at a wavelength of 1278 nm. Attributed to lasing, this threshold behavior occurs at temperatures below 70 K. No such behavior was observed at the secondary emission wavelength of 1135 nm, which originates from the substrate. The emission spectrum measured at a temperature of 10 K supports the threshold behavior. The spectrum narrows when the pump intensity is increased. The mechanism for light emission (1270-nm wavelength) is believed to be from defects on etched silicon surfaces.

In another report, a team consisting of researchers at the University of California, Irvine, and in Taiwan used a junction diode in which the dopants were confined to nanometer-size regions [71]. The results constitute evidence of stimulated emission at room temperature. Optical amplification has not been demonstrated yet, and electrical-to-optical conversion efficiency is low $(\sim 10^{-4})$. Nevertheless, the room-temperature operation and the electrical pumping are very important features that warrant additional studies aimed at reproducing the results and embedding the structure in an optical waveguide or a cavity.

The successful realization of light emission and amplification in optical fibers that are doped with erbium has motivated efforts aimed at Er-doping in silicon. However, silicon is not a good host for Er, resulting in poor emission at room temperature. The reason is believed to be the backtransfer of energy from the excited Er ions to silicon and also the low concentration of Er that can be accommodated by silicon.

Optical fiber is made from SiO_2 (glass), the main constituent of SRO, suggesting that erbium-doped SRO should be considered as the optical gain medium. Erbium exhibits light emission at the technologically important wavelength of 1550 nm, and other rare-earth dopants can be used to achieve emission at different wavelengths [72]. The material can be excited electrically by sandwiching the film between a silicon layer and a metal film (Fig. 10). Applying a voltage to the so-called MOS structure causes electrons to tunnel through the oxide and, in the process, excite erbium atoms. Silicon nanocrystals also get excited and transfer their energy to the nearby erbium ions. Light-emitting diodes (LEDs) with efficiencies of about 10%, as high as commercial GaAs devices, have been reported by STMicroelectronics, Italy, although with much lower maximum output power of tens of microwatts (Fig. 13) [72]. Energetic electrons injected into the oxide (by tunnelling) cause premature device failure (a link between "hot" electrons and device failure is well established in the electronic devices). Initially, it was believed that the presence of silicon nanocrystals increases the emission cross section of erbium. However, it has recently been shown that this is not the case, and the cross section is the same as in Er-doped glass [73]. Nanocrystals thus play a more modest role. By increasing the conductivity of the SiO_2, silicon nanoparticles reduce the required voltage and hence mitigate device degradation and failure over time, albeit at the expense of reduced emission efficiency.

The attractive features of this technology are the emission in the telecommunication band of 1550 nm and the electrical

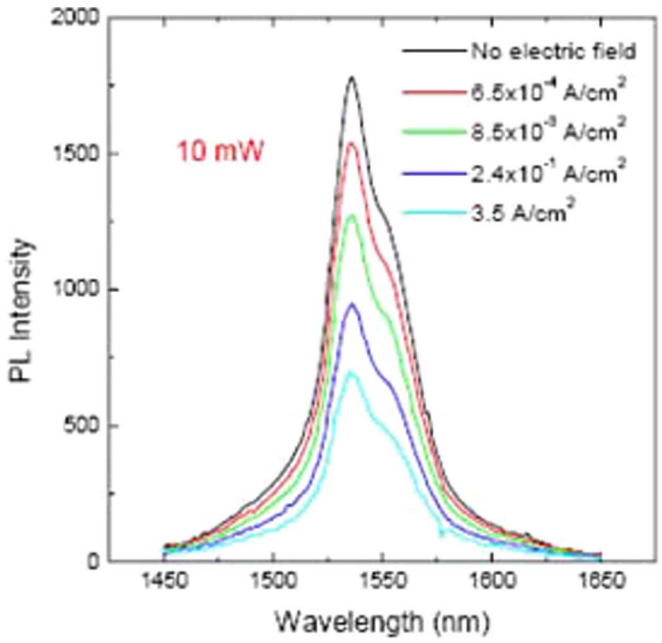

Fig. 14. Dependence of photoluminescence intensity on pump current density in an erbium-doped SRO diode. The reduction in emission with current density may be due to FCA and Auger recombination [74].

pumping. The main challenge that remains in the path to an electrically pumped laser is highlighted in Fig. 14 [74], which shows the dependence of photoluminescence intensity on the pump current density. The emission is observed to diminish with current density, a phenomenon that may be due to FCA and Auger processes, and one that dampens the prospects of achieving electrically pumped amplification and lasing. This effect notwithstanding, another challenge is achieving a high enough current density using a tunnel junction without subjecting the device to excessive heating and premature device failure. To be sure, the highest current density demonstrated in these devices is an order of magnitude lower than the threshold current density in III–V self-assembled quantum dot lasers. Nonetheless, the observation of efficient electrical-to-optical conversion and optically pumped "internal" gain [75] are important developments, and research on means to better understand and overcome the current limitations is underway.

A simpler approach, and one that mimics Er-doped waveguide amplifiers (EDWAs), is the Er-doped glass waveguide, which can be deposited on a silicon substrate. In this case, the material is similar to SRO, except that it contains no nanocrystals. To compensate for the low gain per unit length of Er-doped glass, high-Q-factor microdisk resonators have been used, leading to very low threshold in optically pumped lasers [76].

A near-term approach for realizing a silicon-based laser is the heterogeneous integration of III–V and silicon. Direct growth of GaAs on silicon was extensively studied in the 1980s and has recently attracted renewed interest [77]. A noteworthy recent development is the room-temperature demonstration of an InGaAs quantum dot laser grown directly onto a silicon substrate by Mi *et al.* at the University of Michigan, Ann Arbor [78]. Another recent work is a laser realized by bonding a III–V gain element into a silicon waveguide cavity demonstrated by Park *et al.* at the University of California, Santa Barbara [79]. An electrical version of the laser has been recently demonstrated [80]. A more established technology, and one that has been widely employed for realizing ultracompact optical data transmission modules, is to bond not just the gain element but the complete III–V laser diode (gain element plus high-reflectivity mirrors and metal electrodes) onto a SOI wafer containing silicon waveguide couplers or WDM filters. A recent embodiment is the silicon-based 10-Gb/s optical transceivers by Luxtera Corporation, as discussed earlier [14].

C. Stimulated Raman Scattering (SRS)

The use of SRS in silicon waveguides was proposed in 2002 as a means to realize silicon amplifiers and lasers [81], [82]. This was followed by demonstration of stimulated emission [83] and Raman wavelength conversion [84] in silicon waveguides in 2003. Shortly afterward, the approach led to the demonstration of the first silicon laser in 2004: a device that operated in the pulsed mode [85], [86] followed by demonstration of continuous-wave (CW) lasing in 2005 [87].

Raman backscattering, using primarily visible wavelengths, was used in the late 1960s and early 1970s as an analytical tool to study the vibrational properties of bulk material including silicon [88], [89]. More recently, SRS has been exploited in optical fibers to create amplifiers and lasers. However, several kilometers of fiber is typically required to create a useful device, suggesting that the approach is not applicable to silicon. Often overlooked was the fact that the gain coefficient for SRS in silicon is approximately 10^3-10^4 times higher than that in silica fiber. Additionally, owing to the large refractive index, silicon waveguides can confine the optical field to an area that is approximately 100–1000 times smaller than the modal area in a standard single-mode optical fiber, resulting in proportionally higher Raman gain [81]. When combined, these facts make it possible to observe SRS over the interaction lengths encountered on a chip [81]–[83].

The physics of Raman scattering in silicon waveguides including crystal symmetry considerations has been described elsewhere [90] and will not be repeated here. Instead, a few key features that are necessary for judging the prospects of the technology are summarized.

The Raman scattering process involves the optical phonon branches of atomic vibrations (as opposed to Brillouin, which describes scattering involving acoustic phonons). In the first-order scattering, only one phonon is involved, and momentum conservation implies that only zone-center phonons can participate. Higher order Raman scattering involves multiple phonons, which can be from any point in the Brillouin zone as long as their total momentum equals the (negligible) photon momentum, provided that the selection rules allow it. In silicon, the zone-center optical phonon is triply degenerate with a frequency of 15.6 THz. The first-order resonance, which is of primary importance here, has a full-width at half-maximum of approximately 100 GHz [89]. This imposes a maximum information bandwidth of approximately 100 GHz that can be amplified. The Raman linewidth becomes broader when a broadband pump is used.

The main challenge in silicon Raman devices is the loss caused by the free carriers that are generated via TPA [91], [92]. By determining the steady-state density of generated carriers, and hence the magnitude of the pump-induced loss, the recombination lifetime is the central parameter in Raman as well as other semiconductor nonlinear optical devices. It is well known that the recombination lifetime in SOI is much shorter than that in a bulk silicon sample with comparable doping concentration. This lifetime reduction is due to the presence of interface states at the boundary between the top silicon and the buried oxide layer. This effect depends on the method used for preparation of the SOI wafer and the film thickness, with measured and expected values ranging between 10 and 200 ns [93], [94]. In SOI waveguides, the lifetime is further reduced to a few nanoseconds, or even below in the case of submicrometer waveguides, due to the recombination at the etched waveguide facets and, in the case of rib waveguides, due to diffusion into the slab regions [95], [96]. The lifetime can be further reduced by introducing midgap states through high-energy irradiation and gold or platinum doping. A modest amount of CW gain has been observed in deep-submicrometer waveguides by Espinola *et al.* at Columbia University, New York, NY, [96], where the impact of surface and interface recombination plays a critical role in reducing the lifetime. The carrier density can also be reduced by using a reverse-bias p-n junction to sweep the carriers out [91], [92], and CW gain using this approach has been reported [97], [98]. However, free-carrier screening of the junction electric field, a phenomenon reminiscent of high power saturation in photodetectors, limits the usefulness of this technique to modest pump intensities [99]. Furthermore, the diode results in electrical power being dissipated on the chip. This issue is further discussed in Section VIII.

Being optically pumped, it is unlikely that the Raman laser will play a role in optical interconnects. On the other hand, by compensating for coupling and propagation losses, a Raman amplifier can have an impact. However, the device length will have to be drastically lower than the centimeter-length device demonstrated so far. At an intensity of 100 MW/cm^2 (100-mW pump coupled into a 0.1-μm^2 waveguide) and with silicon's Raman gain coefficient of $\sim$20 cm/GW, the gain will be $\sim$1 dB/mm. Such a modest gain per unit length creates a challenge for miniaturization of Raman amplifiers, a prerequisite for their integration with silicon VLSI-type circuits. The long waveguide length will not be an issue if the device is used as a stand-alone discrete amplifier (similar to the role played by the EDWA). By using cladding pump architecture, it has been shown that these devices can offer extremely high gain [100]. Hence, they may be viewed as a high gain but narrow-band counterpart to the EDWA [100].

Recently, an important laser component, i.e., a saturable absorber, has been demonstrated in silicon by Grawert *et al.* at the Massachusetts Institute of Technology, Cambridge [101]. Realized as a Bragg reflector, the device consisting of a silicon/SiO_2/germanium structure has been used to demonstrate mode locking of an Er–Yb:glass laser. The laser has an ultrabroadband of 700 nm and generates 220-fs pulses. When used with a silicon gain medium, such a device can be used to create all-silicon mode-locked lasers.

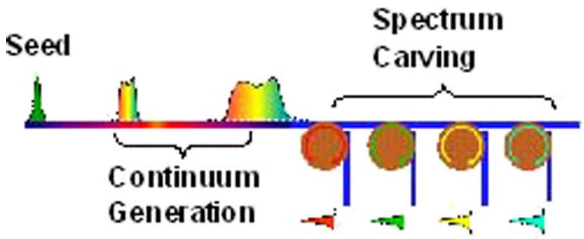

Fig. 15. Schematic depicts how continuum generation from an off-chip seed laser can be integrated with spectral filters for on-chip generation of WDM channels.

VII. Wavelength Conversion and Continuum Generation

Wavelength conversion, a critical function in optical networking, can be performed using both Raman [102]–[104] and Kerr nonlinearities [105]–[107], as well as cross-absorption modulation based on free-carrier generation [108]. In the Raman approach, the Stokes' to anti-Stokes' separation corresponds to approximately 200 nm (twice the 15.6-THz optical phonon frequency) in the telecommunication band. Hence, this approach lends itself to wavelength band conversion between the 1300- and 1500-nm bands, a hypothesis which has been experimentally demonstrated [102], [103]. Because of the large wavelength separation, phase matching is challenging, although it has recently been shown that stress-induced birefringence can be used to cancel the material dispersion and realize phase matching [109]. Kerr effect is ideal for wavelength channel conversion, where the close wavelength spacing alleviates the phase-matching problem. The increase of waveguide dispersion in silicon wires (< 1 μm transverse dimensions) offers another means to achieve phase matching [104], [107]. Furthermore, the concomitant increase in the optical intensity (for a fixed power) in such waveguides enhances the nonlinear interactions and improves the conversion efficiency. Using these concepts, a wavelength channel conversion with gain has been demonstrated by Foster *et al.* [107].

Another requirement for such devices is the response time. The response time for the Raman process is approximately 10 ps and is in the femtosecond range for the Kerr effect, leading to ultrafast conversion for both processes. This is not the case for conversion using free-carrier generation, where the response time is limited to the nanosecond range by the recombination lifetime. Multiwavelength sources will be needed before WDM can be applied to chip-level communication. The lack of an electrically pumped silicon laser, to date, means that external lasers must be coupled onto the chip. This will increase the cost of packaging when several lasers ought to be coupled onto the chip. On-chip generation of a broad continuum from an external seed laser has been proposed as a means to overcome this problem [110], [111]. In this scenario, the generated continuum can be carved using integrated filters, resulting in discrete WDM channels (Fig. 15). A similar approach, but one using continuum generation in fibers, has previously been applied to fiber-optic dense WDM networks [112]. The requisite spectral broadening in both silicon and fiber takes place through self-phase modulation (SPM), experienced by a short pulse with a high peak power. To avoid the strong Raman interaction in

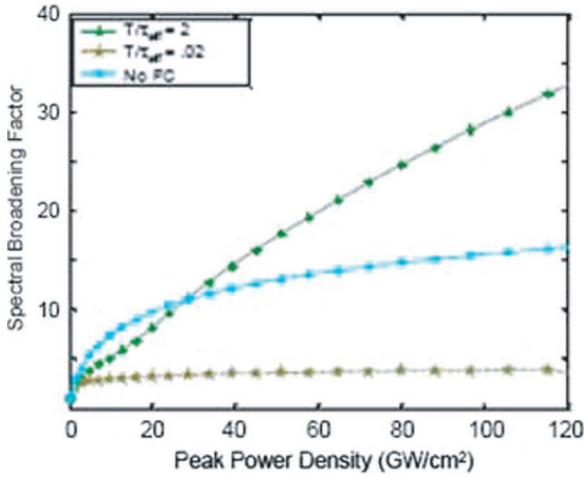

Fig. 16. Broadening factor that can be achieved in silicon versus peak pulse power. SPM occurs due to both the electronic nonlinear response (conventional $\chi^{(3)}$) and TPA-generated free-carrier modulation [111]. For peak intensities less than 20 GW/cm^2, electronic nonlinearity, while for larger intensities, free-carrier index modulation, is the main cause of SPM. T: repletion period of seed laser; τ_{eff}: recombination lifetime.

silicon, the pulsewidth ($\sim$1 ps) is kept shorter than the characteristic response time of optical phonons [110]. With a Raman linewidth of 100 GHz in silicon, the latter is about 10 ps. Fig. 16 shows the broadening factor that can be achieved in silicon versus peak pulse power. SPM occurs due to both the electronic nonlinear response (conventional $\chi^{(3)}$) and TPA-generated free-carrier modulation [111]. To demonstrate the competing contributions of these two mechanisms, the results are provided for different ratios of T/τ_{eff}, where T is the repetition period of the seed laser and τ_{eff} is the recombination lifetime. For peak intensities less than 20 GW/cm^2, electronic nonlinearity dominates, resulting in a continuum spectrum that is symmetric about the seed wavelength. For larger intensities, free-carrier index modulation is the main cause of SPM. Since the free-carrier-induced phase shift is proportional to the carrier density, the trailing edge of the pulse sees a higher phase shift than the leading edge. This gives rise to a continuum that has an asymmetric spectrum. Recently, spectrum broadening has also been demonstrated in waveguides with submicrometer cross sections, where the increase in optical intensity reduces the required power for the seed laser [113].

VIII. Road Ahead: Economic Challenges and Heat Compatibility Issues

The prevailing vision for silicon photonics has been the introduction of photonics into the silicon CMOS manufacturing process. This vision has been motivated by the compatibility of silicon photonics with the CMOS process. To uncover what challenges lie ahead, one is well advised to probe the full implication of "compatibility." The "compatibility–quad," as shown in Fig. 17, describes the full extent of this requirement. Among the four constituents of compatibility, "material" and "process" compatibilities are self-explanatory and are much easier to satisfy than "economic" and "heat" compatibilities. In the following, we will discuss the latter two.

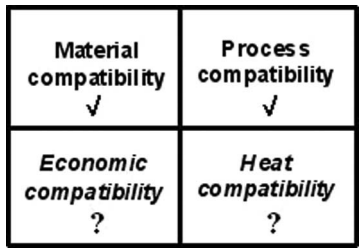

Fig. 17. Compatibility–quad describing conditions that must be met by silicon photonics to be fully compatible with VLSI electronics. Material and process compatibilities are self-explanatory and are readily satisfied. Economic compatibility dictates highly efficient use of wafer real estate and products that have a high-volume market. Heat compatibility requires that photonic devices must be able to operate on the hot VLSI substrate and that their own power dissipation should be negligible.

Efficient use of wafer real estate is what fuels the relentless scaling of CMOS to smaller feature lengths. For photonics to merge with VLSI electronics, it cannot significantly increase the chip area; otherwise, it will violate the economics of silicon manufacturing. The use of silicon wire waveguides with 100–1000 nm transverse dimensions (popularly known as "nanophotonics") partially addresses this requirement. However, the ultimate answer to economic compatibility will be the three-dimensional (3-D) integration of electronics and photonics, a preliminary example of which has recently been demonstrated (Fig. 18) [114], [115]. This approach employs multilayer SOI architecture in which the photonic devices are first formed in the buried silicon layer (using patterned oxygen implantation). The surface silicon layer is then used for conventional CMOS processing. Another requirement for economic compatibility is that the products must have a high-volume market. In this case, the large nonrecurring engineering cost of the state-of-the-art CMOS process is amortized among the large number of devices sold, resulting in a low per-unit cost. In other words, being CMOS based does not necessarily translate into low cost. It does so only if the product has a high volume market.

Fig. 19 shows the alarming increase in power density of VLSI chips, where today's level of 100 W/cm^2 challenges even the most advanced packaging technologies [116]. The problem of heat dissipation is so severe that it threatens to bring to halt the continued advance of the technology, as described by Moore's law [117]. This fact is highlighted by the recent momentous shift of the microprocessor industry away from increasing the clock speed and in favor of multicore processors [118]. Among photonic components, lasers are the most power-hungry photonic devices. The lack of an electrically pumped Si laser, to date, dictates an architecture where the light source (also known as "optical power supply") remains off-chip. Far from being a compromised solution, this architecture is in fact preferred as it removes a main source of heat dissipation. Furthermore, the performance degradation of injection lasers at high temperatures will be a major obstacle to their integration onto the hot VLSI substrate, even when such silicon lasers are demonstrated. Nevertheless, creating an electrically pumped silicon laser or a practical LED is a worthy goal as such devices can impact other applications, such as optoelectronic displays and lighting.

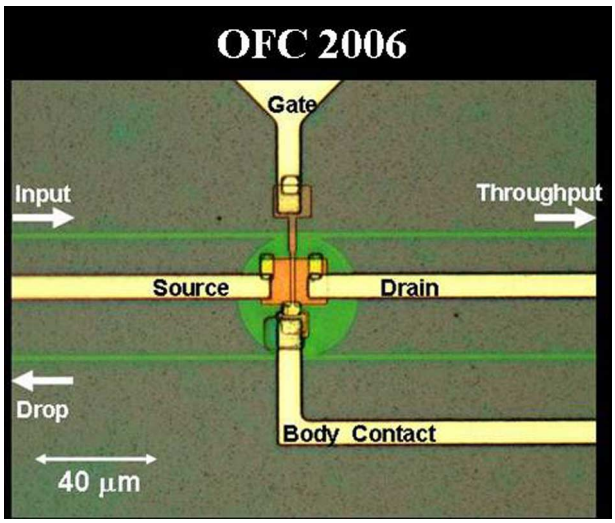

Fig. 18. Ultimate solution to efficient use of wafer real estate is 3-D integration of electronics on top of buried photonics. The example shown here is a MOS transistor fabricated on top of a subsurface microdisk resonator. The fully monolithic process employs multilayers of SOI, formed by patterned oxygen implantation, in which photonic devices are first formed in the buried silicon layer [114].

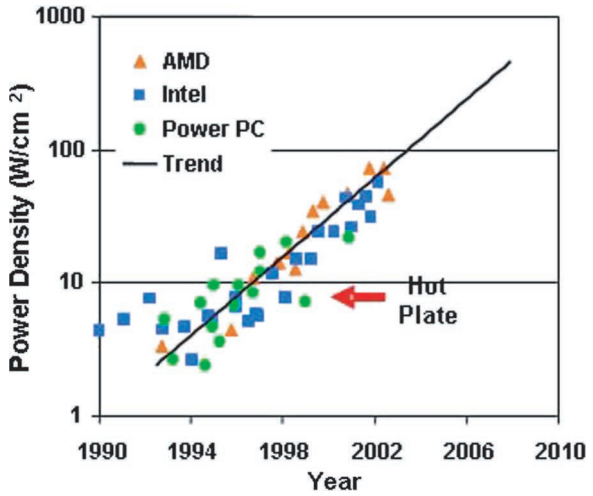

Fig. 19. Alarming increase in power density of VLSI chips [116]. The problem of heat dissipation resulted in the recent shift of the microprocessor industry away from increasing the clock speed and in favor of multicore processors [118]. The figure highlights the fact that photonic devices must be able to operate on the hot VLSI substrate and that their own power dissipation must be minimal (figure courtesy of E. Pop).

Modulators, amplifiers, photodetectors, and perhaps wavelength converters are destined to be integrated on-chip. Among these devices, the modulator and the amplifier have the highest power dissipation. Similar to bipolar transistors, carrier-injection-type optical modulators suffer from static power dissipation. On the other hand, depletion-mode free-carrier modulators, as well as those based on the quantum-confined Stark effect in Si/Ge quantum wells [119], will have negligible static power dissipation. Kuo *et al.* from Stanford University, Stanford, CA, have recently demonstrated strong electrooptic modulation in Si/Ge quantum wells, comparable to what is achieved in GaAs/AlGaAs structures [120]. This approach

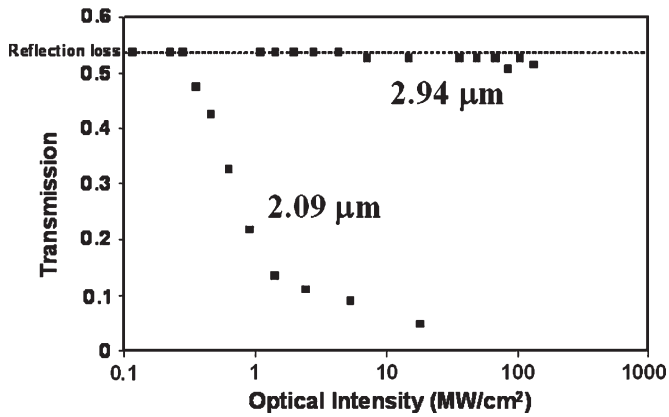

Fig. 20. Measured nonlinear absorption in silicon in the mid-IR. Two-photon carrier generation and the resulting free-carrier loss vanish when the pump wavelength is above ~2.25 μm, i.e., the two-photon band edge [124].

promises a new class of silicon modulators that resemble the III–V electroabsorption modulators.

To date, the Raman approach is the only proven candidate for optical amplification in silicon. As mentioned earlier, to overcome nonlinear losses, a reverse bias p-n junction is used to remove the free carriers. This solution can come at the expense of a large amount of heat being dissipated onto the chip. In [87], about 1 W of electrical power had to be dissipated (25 V at ~40 mA) to achieve ~4 dB of CW optical gain and to produce ~8 mW of output from the Raman laser. Recently, it has been demonstrated that similar values of CW gain can be obtained at zero bias resulting in zero power dissipation [98]. Moving beyond this, it was also shown that it is even possible to obtain CW optical gain while harvesting electrical power from the device [121], [122]. In this mode, the TPA-generated carriers are swept out by the built-in field of the junction; yet, the device delivers electrical power. The concept becomes clear if one considers the device as a nonlinear optical equivalent of a solar cell [121], [122]. To the extent that TPA generation occurs in other semiconductor nonlinear photonic devices (such as wavelength converters), the approach is applicable to those devices as well. This approach works at low-to-moderate pump intensities, beyond which the junction electric field is unable to sweep out the free carriers, leading to an optical loss [99].

Managing the TPA-induced FCA is the fundamental challenge in devices that take advantage of the third-order nonlinear interactions (wavelength converters, Raman amplifiers, etc.) because high optical intensities are needed to induce nonlinear interactions. To this end, lifetime reduction techniques that are used in producing silicon step recovery diodes and fast photoconductors, such as gold or platinum doping, as well as particle beam irradiation, may produce benefits. On this note, modest CW gain has been demonstrated using helium implantation [123].

Fortunately, the TPA problem vanishes altogether in mid-IR wavelengths. Fig. 20 shows measurements of nonlinear loss in the mid-IR [124]. Two-photon carrier generation disappears beyond the two-photon band edge (2.25-μm wavelength). This, along with excellent passive transmission (Fig. 1), renders silicon an excellent optical crystal for the midwave IR

TABLE I
COMPARISON OF VARIOUS RAMAN SOLID-STATE LASER MATERIALS WITH SILICON [12]

Properties of Raman media	Silicon	$Ba(NO_3)_2$	$LiIO_3$	$KGd(WO_4)_2$	$CaWO_4$
Trasmission Range (μm)	1.1-6.5	0.38-1.8	0.38-5.5	0.35-5.5	0.2-5.3
Refractive index	3.42	1.556	1.84 (o) 1.711 (e)	1.986 p[mm]p 2.033 p[gg]p	1.884 (o) 1.898 (e)
Raman shift at 300K (cm^{-1})	521	1047.3	770 822	901 768	910.7
Spontaneous Raman linewidth (cm^{-1})	3.5	0.4	5.0	5.9	4.8
Raman gain (cm/GW)	20 (1550nm)	11 (1064nm)	4.8 (1064nm)	3.3 (1064)	-
Optical damage threshold (MW/cm^2)	~1000-4000	~400	~100	-	-
Thermal conductivity (W/m-K)	148	1.17	-	2.6 [1 0 0] 3.8 [0 1 0] 3.4 [0 0 1]	16

spectrum (wavelengths 2–6 μm) where important applications exist, ranging from biochemical detection to laser imaging detection and ranging, as well as free space optical communications [12]. While there are a number of solid-state crystals that are excellent Raman media, a comparison of relevant material parameters indicates that silicon rates quite favorably with these (Table I) [12]. Silicon's mature technology for fabrication of waveguides and resonators is an additional advantage.

Propagation loss is a fundamental parameter that impacts virtually all silicon photonic devices. As pointed out earlier, good progress has been made in improving the morphology of silicon surface by oxidation. Additionally, high-temperature annealing in hydrogen ambient has been shown to improve the surface morphology (Fig. 21), although the dramatic structural improvement has not yet produced the lowest losses [125]. Recognizing that some of the roughness in etched structures originates from the nonsmooth edges of the photoresist pattern that is used as the etch mask, resist reflow has been used to improve the surface morphology [126]. Using this technique to create highly circular disks patterns, a propagation loss of 0.1 dB/cm has been deduced from the measured high-quality factor (Q) of microdisk resonators, a value that has been attributed to surface-state absorption [126]. This indicates that, similar to the case of electronic devices, surface effects will impact the performance of scaled silicon photonic devices, and going forward, surface passivation techniques will play an increasingly important role in silicon photonics.

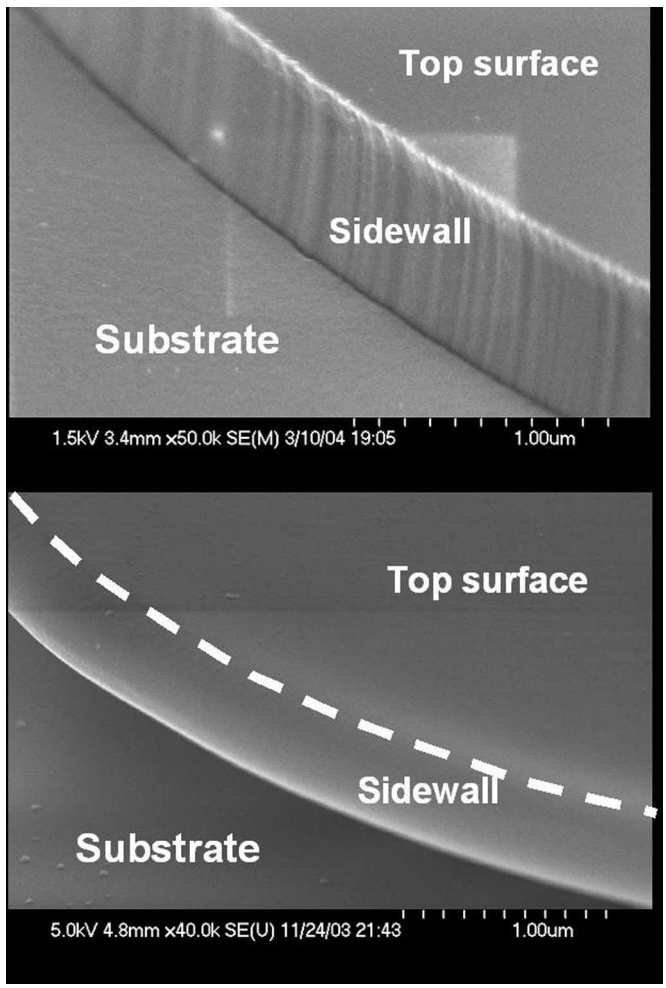

Fig. 21. Impact of high-temperature hydrogen annealing on the morphology of an etched silicon sidewall for a microdisk resonator (figure courtesy of M. C. Wu) [125].

IX. CLOSING REMARKS

This paper has been an attempted overview of the silicon photonics application space, the current state of device technology, and the challenges that lie ahead on the path to commercial success.

The burgeoning of the field over the last five years has made it all but impossible to provide a comprehensive coverage of the numerous worldwide efforts that are advancing the state of the art. Recognizing this limitation, the present authors have had to limit the scope of this paper. For instance, generation of light using iron disilicide [127], dislocation loops [128], and high-purity textured silicon [129] was not discussed.

Most prominently, photonic band structure devices were not discussed in this paper, although they represent a major subfield within silicon photonics. The high index contrast of Si/SiO_2 and Si/air renders SOI the ideal platform for such devices. Photonic crystals have tremendous potential as is evidenced by recent demonstrations of unique functionalities, such as cavities with ultrasmall mode volumes [130], the superprism effect [131], [132], self-guiding or the so-called supercollimation [133], ultracompact waveguide bends [134], and slow light [135]. Its tremendous potential notwithstanding, the main drawback of the photonic crystal approach is the large optical loss encountered in deeply etched periodic structures, which is an attribute that arises from the abundance of surfaces and the concomitant prominence of surface scattering. Another limitation is the sensitivity to fabrication-induced errors in device geometry. A cautionary case study that may underscore this point is photonic crystal fibers, whose promise of replacing standard fibers was not realized due to losses associated with surface effects. On a more optimistic note, photonic crystal fibers have found other applications such as high dispersive elements in the form of hollow-core fibers and compact cavities that can be filled with a wide range of optically active gasses or liquids. Hence, it is rather likely that a silicon-based photonic crystal device will play a role by providing functionalities that are not offered by traditional integrated optical devices.

ACKNOWLEDGMENT

The authors would like to thank Dr. J. Shah of DARPA for his visionary support of silicon photonics.

REFERENCES

[1] R. Soref and J. Lorenzo, "All-silicon active and passive guided-wave components for $\lambda = 1.3$ and 1.6 μm," *IEEE J. Quantum Electron.*, vol. QE-22, no. 6, pp. 873–879, Jun. 1986.

[2] R. A. Soref and B. R. Bennett, "Kramers–Kronig analysis of E–O switching in silicon," in *Proc. SPIE Integr. Opt. Circuit Eng.*, 1986, vol. 704, pp. 32–37.

[3] B. Schuppert, J. Schmidtchen, and K. Petermann, "Optical channel waveguides in silicon diffused from GeSi alloy," *Electron. Lett.*, vol. 25, no. 22, pp. 1500–1502, Oct. 1989.

[4] R. A. Soref, J. Schmidtchen, and K. Petermann, "Large single-mode rib waveguides in GeSi and Si-on-SiO_2," *IEEE J. Quantum Electron*, vol. 27, no. 8, pp. 1971–1974, Aug. 1991.

[5] P. D. Trinh, S. Yegnanarayanan, and B. Jalali, "Integrated optical directional couplers in silicon-on-insulator," *Electron. Lett.*, vol. 31, no. 24, pp. 2097–2098, Nov. 1995.

[6] U. Fischer, T. Zinke, and K. Petermann, "Integrated optical waveguide switches in SOI," in *Proc. IEEE Int. SOI Conf.*, Oct. 1995, pp. 141–142.

[7] T. T. H. Eng, S. S. Y. Sin, S. C. Kan, and G. K. L. Wong, "Surface micromachined movable SOI optical waveguides," in *Proc. Int. Conf. Solid-State Sens. Actuators*, 1995, vol. 1, pp. 348–350.

[8] C. Z. Zhao, G. Z. Li, E. K. Liu, Y. Gao, and X. D. Liu, "Silicon on insulator Mach–Zehnder waveguide interferometers operating at 1.3 μm," *Appl. Phys. Lett.*, vol. 67, no. 17, pp. 2448–2449, Oct. 1995.

[9] P. D. Trinh, S. Yegnanarayanan, and B. Jalali, "5 $\times$ 9 integrated optical star coupler in silicon-on-insulator technology," *IEEE Photon. Technol. Lett.*, vol. 8, no. 6, pp. 794–796, Jun. 1996.

[10] P. D. Trinh, S. Yegnanarayanan, F. Coppinger, and B. Jalali, "Silicon on-insulator (SOI) phased-array wavelength multi-demultiplexer with extremely low-polarization sensitivity," *IEEE Photon. Technol. Lett.*, vol. 9, no. 7, pp. 940–942, Jul. 1997.

[11] B. Jalali, S. Yegnanarayanan, T. Yoon, T. Yoshimoto, I. Rendina, and F. Coppinger, "Advances in silicon-on-insulator optoelectronics," *IEEE J. Sel. Topics Quantum Electron.*, vol. 4, no. 6, pp. 938–947, Nov./Dec. 1998.

[12] B. Jalali, V. Raghunathan, R. Shori, S. Fathpour, D. Dimitropoulos, and O. Stafsudd, "Prospects for silicon mid-IR Raman lasers," *IEEE J. Sel. Topics Quantum Electron.,* submitted for publication.

[13] Kotura Inc. products. [Online]. Available: http://www.kotura.com/

[14] C. Gunn, "CMOS photonics for high-speed interconnects," *IEEE Micro*, vol. 26, no. 2, pp. 58–66, Mar./Apr. 2006.

[15] D. A. B. Miller, "Optical interconnects to silicon," *IEEE J. Sel. Topics Quantum Electron.*, vol. 6, no. 6, pp. 1312–1317, Nov./Dec. 2000.

[16] D. Pham, S. Asano, M. Bolliger, M. N. Day, H. P. Hofstee, C. Johns, J. Kahle, A. Kameyama, J. Keaty, Y. Masubuchi, M. Riley, D. Shippy, D. Stasiak, M. Suzuoki, M. Wang, J. Warnock, S. Weitzel, D. Wendel, T. Yamazaki, and K. Yazawa, "The design and implementation of a first-generation CELL processor," in *Proc. IEEE Int. Solid-State Circuits Conf. Dig. Tech. Papers*, Feb. 2005, vol. 1, pp. 184–592.

[17] K. Chang, S. Pamarti, K. Kaviani, E. Alon, X. Shi, T. J. Chin, J. Shen, G. Yip, C. Madden, R. Schmitt, C. Yuan, F. Assaderaghi, and M. Horowitz, "Clocking and circuit design for a parallel I/O on a first-generation CELL processor," in *Proc. IEEE Int. Solid-State Circuits Conf. Dig. Tech. Papers*, Feb. 2005, vol. 1, pp. 526–615.

[18] N. M. Jokerst, M. A. Brooke, S. Cho, M. Thomas, J. Lillie, D. Kim, S. Ralph, and K. Dennis, "Integrated planar lightwave bio/chem OEIC sensors on Si CMOS circuits," *Proc. SPIE*, vol. 5730, pp. 226–233, 2005.

[19] J. J. Saarinen, J. E. Sipe, S. M. Weiss, and P. M. Fauchet, "Optical sensors based on resonant porous silicon structures," *Opt. Express*, vol. 13, no. 10, pp. 3754–3764, May 2005.

[20] J. Takahashi, T. Tsuchizawa, T. Watanabe, and S. Itabashi, "Oxidation-induced improvement in the sidewall morphology and cross-sectional profile of silicon wire waveguides," *J. Vac. Sci. Technol. B, Microelectron. Process. Phenom.*, vol. 22, no. 5, pp. 2522–2525, Sep. 2004.

[21] Y. Vlasov and S. McNab, "Losses in single-mode silicon-on-insulator strip waveguides and bends," *Opt. Express*, vol. 12, no. 8, pp. 1622–1631, Apr. 2004.

[22] T. Tsuchizawa, K. Yamada, H. Fukuda, T. Watanabe, J. Takahashi, M. Takahashi, T. Shoji, E. Tamechika, S. Itabashi, and H. Morita, "Microphotonic devices based on silicon microfabrication technology," *IEEE J. Sel. Topics Quantum Electron.*, vol. 11, no. 1, pp. 232–240, Jan./Feb. 2005.

[23] K. Yamada, T. Shoji, T. Tsuchizawa, T. Watanabe, J. Takahashi, and S. Itabashi, "Silicon-wire-based ultrasmall lattice filters with wide free spectral ranges," *Opt. Lett.*, vol. 28, no. 18, pp. 1663–1664, Sep. 2003.

[24] S. McNab, N. Moll, and Y. Vlasov, "Ultra-low loss photonic integrated circuit with membrane-type photonic crystal waveguides," *Opt. Express*, vol. 11, no. 22, pp. 2927–2939, Nov. 2003.

[25] V. R. Almeida, R. R. Panepucci, and M. Lipson, "Nano-taper for compact mode conversion," *Opt. Lett.*, vol. 28, no. 15, pp. 1302–1304, Aug. 2003.

[26] G. Roelkens, P. Dumon, W. Bogaerts, D. Van Thourhout, and R. Baets, "Efficient fiber to SOI photonic wire coupler fabricated using standard CMOS technology," in *Proc. 18th Annu. Meeting IEEE LEOS*, Oct. 2005, pp. 214–215.

[27] D. Taillaert, W. Bogaerts, P. Bienstman, T. F. Krauss, P. Van Daele, I. Moerman, S. Verstuyft, K. De Mesel, and R. Baets, "An out-of-plane grating coupler for efficient butt-coupling between compact planar waveguides and single-mode fibers," *IEEE J. Quantum Electron.*, vol. 38, no. 7, pp. 949–955, Jul. 2002.

[28] A. Narasimha, "Low dispersion, high spectral efficiency, RF photonic transmission systems and low loss grating couplers for silicon-on-insulator nanophotonic integrated circuits," Ph.D. dissertation, Univ. California, Los Angeles, 2004.

[29] P. Koonath, T. Indukuri, and B. Jalali, "Add–drop filters utilizing vertically-coupled microdisk resonators in silicon," *Appl. Phys. Lett.*, vol. 86, no. 9, pp. 091102(1)–091102(3), Mar. 2005.

[30] M. M. Lee and M. C. Wu, "MEMS-actuated microdisk resonators with variable power coupling ratios," *IEEE Photon. Technol. Lett.*, vol. 17, no. 5, pp. 1034–1036, May 2005.

[31] M. A. Popovic, T. Barwicz, M. R. Watts, P. T. Rakich, L. Socci, E. P. Ippen, F. X. Kärtner, and H. I. Smith, "Multistage high-order

microring-resonator add–drop filters," *Opt. Lett.*, vol. 31, no. 17, pp. 2571–2573, Sep. 2006.
[32] R. A. Soref and B. R. Bennett, "Electrooptical effects in silicon," *IEEE J. Quant. Electronics*, vol. QE-23, no. 1, pp. 123–129, Jan. 1987.
[33] J. P. Lorenzo and R. A. Soref, "1.3 μm electro-optic silicon switch," *Appl. Phys. Lett.*, vol. 5, no. 1, pp. 6–8, Jul. 1987.
[34] L. Friedman, R. A. Soref, and J. P. Lorenzo, "Silicon double-injection electro-optic modulator with junction gate control," *J. Appl. Phys.*, vol. 63, no. 6, pp. 1831–1839, Mar. 1988.
[35] S. R. Giguere, L. Friedman, R. A. Soref, and J. P. Lorenzo, "Simulation studies of silicon electro-optic waveguide devices," *J. Appl. Phys.*, vol. 68, no. 10, pp. 4964–4970, Nov. 1990.
[36] C. K. Tang, G. T. Reed, A. J. Walton, and A. G. Rickman, "Simulation of a low loss optical modulator for fabrication in SIMOX material," in *Proc. Mater. Res. Soc. Symp.*, 1993, vol. 298, pp. 247–252.
[37] ——, "Low-loss, single-mode, optical phase modulator in SIMOX material," *J. Lightw. Technol.*, vol. 12, no. 8, pp. 1394–1400, Aug. 1994.
[38] C. K. Tang and G. T. Reed, "Highly efficient optical phase modulator in SOI waveguides," *Electron. Lett.*, vol. 31, no. 6, pp. 451–452, Mar. 1995.
[39] G. T. Reed and C. E. Png, "Silicon optical modulators," *Mater. Today*, vol. 8, no. 1, pp. 40–50, Jan. 2005.
[40] L. Liao, D. Samara-Rubio, M. Morse, A. Liu, D. Hodge, D. Rubin, U. Keil, and T. Franck, "High speed silicon Mach–Zehnder modulator," *Opt. Express*, vol. 13, no. 8, pp. 3129–3135, Apr. 2005.
[41] EOspcase Inc., *10-20 Gb/s Modulators.* [Online]. Available: http://www.eospace.com/12.5+G_modulator.htm
[42] C. E. Png, G. T. Reed, W. R. Headley, K. P. Homewood, A. Liub, M. Paniccia, R. M. H. Atta, G. Ensell, A. G. R. Evans, D. Hak, and O. Cohen, "Design and experimental results of small silicon-based optical modulators," *Proc. SPIE*, vol. 5356, pp. 44–55, 2004.
[43] G. Cocorullo, A. Cutolo, F. G. Della Corte, and I. Rendina, "New possibilities for efficient silicon integrated electro-optical modulators," *Opt. Commun.*, vol. 86, no. 2, pp. 228–235, Nov. 1991.
[44] V. R. Almeida, C. A. Barrios, R. Panepucci, and M. Lipson, "All-optical control of light on a silicon chip," *Nature*, vol. 431, no. 7012, pp. 1081–1084, Oct. 2004.
[45] Q. Xu, B. Shmidt, S. Pradhan, and M. Lipson, "Micrometre-scale silicon electro-optic modulator," *Nature*, vol. 435, no. 7040, pp. 325–327, May 2005.
[46] O. Boyraz and B. Jalali, "Demonstration of a directly modulated silicon Raman laser," *Opt. Express*, vol. 13, no. 3, pp. 796–800, Feb. 2005.
[47] D. Wood, *Optoelectronic Semiconductor Devices*. Trowbridge, U.K.: Prentice-Hall, 1994, p. 250.
[48] H. Temkin, J. C. Bean, T. P. Pearsall, N. A. Olsson, and D. V. Lang, "High photoconductive gain in Ge_xSi_{1-x}/Si strained-layer superlattice detectors operating at 1.3 μm," *Appl. Phys. Lett.*, vol. 49, no. 3, pp. 155–157, Jul. 1986.
[49] B. Jalali, A. F. J. Levi, F. Ross, and E. A. Fitzgerald, "SiGe waveguide photodetectors grown by rapid thermal chemical vapour deposition," *Electron. Lett.*, vol. 28, no. 3, pp. 269–271, Jan. 1992.
[50] B. Jalali, L. Naval, and A. F. J. Levi, "Si-based receivers for optical data links," *J. Lightw. Technol.*, vol. 12, no. 6, pp. 930–935, Jun. 1994.
[51] F. Y. Huang, K. Sakamoto, K. L. Wang, P. Trinh, and B. Jalali, "Epitaxial SiGeC waveguide photodetector grown on Si substrate with response in the 1.3–1.55-μm wavelength range," *IEEE Photon. Technol. Lett.*, vol. 9, no. 2, pp. 229–231, Feb. 1997.
[52] L. Colace, G. Masini, and G. Assanto, "Ge-on-Si approach to the detection of near-infrared light," *IEEE J. Quantum Electron*, vol. 35, no. 12, pp. 1843–1852, Dec. 1999.
[53] J. Michel, J. F. Liu, W. Giziewicz, D. Pan, K. Wada, D. D. Cannon, S. Jongthammanurak, D. T. Danielson, L. C. Kimerling, J. Chen, F. O. Ilday, F. X. Kartner, and J. Yasaitis, "High performance Ge p-i-n photodetectors on Si," in *Proc. Group IV Photon. Conf.*, Sep. 2005, pp. 177–179.
[54] S. M. Csutak, J. D. Schaub, S. Wang, J. Mogab, and J. C. Campbell, "Integrated silicon optical receiver with avalanche photodiode," *Proc. Inst. Electron. Eng.—Optoelectron.*, vol. 150, no. 3, pp. 235–237, Jun. 2003.
[55] G. Dehlinger, J. D. Schaub, S. J. Koester, Q. C. Ouyang, J. O. Chu, and A. Grill, "High-speed germanium-on-insulator photodetectors," in *Proc. 18th Annu. Meeting IEEE LEOS*, Oct. 2005, pp. 321–322.
[56] M. Jutzi, M. Berroth, G. Wohl, M. Oehme, and E. Kasper, "Ge-on-Si vertical incidence photodiodes with 39-GHz bandwidth," *IEEE Photon. Technol. Lett.*, vol. 17, no. 7, pp. 1510–1512, Jul. 2005.
[57] C. L. Schow, L. Schares, S. J. Koester, G. Dehlinger, R. John, and F. E. Doany, "A 15-Gb/s 2.4-V optical receiver using a Ge-on-SOI photodiode and a CMOS IC," *IEEE Photon. Technol. Lett.*, vol. 18, no. 19, pp. 1981–1983, Oct. 2006.
[58] D. J. Ripin, C. Chudoba, J. T. Gopinath, J. G. Fujimoto, E. P. Ippen, U. Morgner, F. X. Kärtner, V. Scheuer, G. Angelow, and T. Tschudi, "Generation of 20-fs pulses by a prismless Cr^{4+} : YAG laser," *Opt. Lett.*, vol. 27, no. 1, pp. 61–63, Jan. 2002.
[59] C. Xu, J. M. Roth, W. H. Knox, and K. Bergman, "Light with single photon counting silicon avalanche photodiode," *Electron. Lett.*, vol. 38, no. 2, pp. 86–88, Jan. 2002.
[60] R. Salem, G. E. Tudury, T. U. Horton, G. M. Carter, and T. E. Murphy, "Polarization-insensitive optical clock recovery at 80 Gb/s using a silicon photodiode," *IEEE Photon. Technol. Lett.*, vol. 17, no. 9, pp. 1968–1970, Sep. 2005.
[61] Y. Liu, C. W. Chow, W. Y. Cheung, and H. K. Tsang, "In-line channel power monitor based on helium ion implantation in silicon-on-insulator waveguides," *IEEE Photon. Technol. Lett.*, vol. 18, no. 17, pp. 1882–1884, Sep. 2006.
[62] B. Jalali, D. Dimitropoulos, V. Raghunathan, and S. Fathpour, "Silicon lasers," in *Silicon Photonics: State of the Art*, G. Reed, Ed. Hoboken, NJ: Wiley, 2006.
[63] L. Pavesi and G. Guillot, *Optical Interconnects: The Silicon Approach*. Springer Series in Optical Sciences. New York: Springer-Verlag, 2006.
[64] A. Irrera, D. Pacifici, M. Miritello, G. Franzo, F. Priolo, F. Iacona, D. Sanfilippo, G. Di Stefano, and P. G. Fallica, "Electroluminescence properties of light emitting devices based on silicon nanocrystals," *Physica E*, vol. 16, no. 3/4, pp. 395–399, Mar. 2003.
[65] R. J. Walters, G. I. Bourianoff, and A. Atwater, "Field-effect electroluminescence in silicon nanocrystals," *Nat. Mater.*, vol. 4, no. 2, pp. 143–146, Feb. 2005.
[66] L. Pavesi, L. Dal Negro, C. Mazzoleni, G. Franzo, and F. Priolo, "Optical gain in silicon nanocrystals," *Nature*, vol. 408, no. 6811, pp. 440–444, Nov. 2000.
[67] J. Ruan, P. M. Fauchet, L. Dal Negro, M. Cazzanelli, and L. Pavesi, "Stimulated emission in nanocrystalline silicon superlattices," *Appl. Phys. Lett.*, vol. 83, no. 26, pp. 5479–5481, Dec. 2003.
[68] P. M. Fauchet, "Light emission from Si quantum dots," *Materials Today*, vol. 8, no. 1, pp. 23–26, Jan. 2005.
[69] L. Pavesi, "Routes towards silicon-based lasers," *Mater. Today*, vol. 8, no. 1, pp. 23–26, Jan. 2005.
[70] S. G. Cloutier, P. A. Kossyrev, and J. Xu, "Optical gain and stimulated emission in periodic nanopatterned crystalline silicon," *Nat. Mater.*, vol. 4, no. 12, pp. 887–891, Dec. 2005.
[71] M. J. Chen, J. L. Yen, J. Y. Li, J. F. Chang, S. C. Tsai, and C. S. Tsai, "Stimulated emission in a nanostructured silicon pn junction diode using current injection," *Appl. Phys. Lett.*, vol. 84, no. 12, pp. 2163–2165, Mar. 2004.
[72] M. E. Castagna, S. Coffa, L. Carestia, A. Messian, and C. Buongiorno, "Quantum dot materials and devices for light emission in silicon," presented at the 32nd Eur. Solid-State Device Research Conf. (ESSDERC), Firenze, Italy, 2002, Paper D21.3.
[73] H. Mertens, A. Polman, I. M. P. Aarts, W. M. M. Kessels, and M. C. M. van de Sanden, "Absence of the enhanced intra-4f transition cross section at 1.5 μm of Er^{3+} in Si-rich SiO_2," *Appl. Phys. Lett.*, vol. 86, no. 24, p. 241109, Jun. 2005.
[74] C. D. Presti, A. Irrera, G. Franzò, F. Priolo, F. Iacona, D. Sanfilippo, G. Di Stefano, A. Piana, and P. G. Fallica, "Light emitting devices based on silicon nanoclusters," in *Proc. 2nd IEEE Int. Conf. Group IV Photon.*, 2005, pp. 45–47.
[75] J. Lee, J. H. Shin, and N. Park, "Optical gain at 1.5 μm in nanocrystal Si-sensitized Er-doped silica waveguide using top-pumping 470 nm LEDs," *J. Lightw. Technol.*, vol. 23, no. 1, pp. 19–25, Jan. 2005.
[76] A. Polman, B. Min, J. Kalkman, T. J. Kippenberg, and K. J. Vahala, "Ultra-low threshold erbium-implanted toroidal microlaser on silicon," *Appl. Phys. Lett.*, vol. 84, no. 7, pp. 1037–1039, Feb. 2004.
[77] M. T. Bulsara, "Optical interconnects promised by III–V on-silicon integration," *Solid State Technology*, vol. 47, no. 8, p. 22, Aug. 2004.
[78] Z. Mi, P. Bhattacharya, J. Yang, and K. P. Pipe, "Room-temperature self-organized $In_{0.5}Ga_{0.5}As$ quantum dot laser on silicon," *Electron. Lett.*, vol. 41, no. 13, pp. 742–744, Jun. 2005.
[79] H. Park, A. W. Fang, S. Kodama, and J. E. Bowers, "Hybrid silicon evanescent laser fabricated with a silicon waveguide and III–V offset quantum wells," *Opt. Express*, vol. 13, no. 23, pp. 9460–9464, Nov. 2005.
[80] Intel Inc., *Hybrid silicon laser*. [Online]. Available: http://www.intel.com/research/platform/sp/hybridlaser.htm#top

[81] R. Claps, D. Dimitropoulos, Y. Han, and B. Jalali, "Observation of Raman emission in silicon waveguides at 1.54 μm," *Opt. Express*, vol. 10, no. 22, pp. 1305–1313, Nov. 2002.

[82] OSA Press Room Editorial. *Advancing the science of light*. [Online]. Available: http://www.osa.org/news/pressroom/release/11.2002/jalali.aspx

[83] R. Claps, D. Dimitropoulos, V. Raghunathan, Y. Han, and B. Jalali, "Observation of stimulated Raman scattering in silicon waveguides," *Opt. Express*, vol. 11, no. 15, pp. 1731–1739, Jul. 2003.

[84] R. Claps, V. Raghunathan, D. Dimitropoulos, and B. Jalali, "Anti-stokes Raman conversion in silicon waveguides," *Opt. Express*, vol. 11, no. 22, pp. 2862–2872, Nov. 2003.

[85] O. Boyraz and B. Jalali, "Demonstration of a silicon Raman laser," *Opt. Express*, vol. 12, no. 21, pp. 5269–5273, Oct. 2004.

[86] Nature News Editorial. *First silicon laser pulses with life*. [Online]. Available: http://www.nature.com/news/2004/041025/full/041025-10.html

[87] H. Rong, R. Jones, A. Liu, O. Cohen, D. Hak, A. Fang, and M. Pannicia, "A continuous-wave Raman silicon laser," *Nature*, vol. 433, no. 7027, pp. 725–728, Feb. 2005.

[88] J. M. Ralston and R. K. Chang, "Spontaneous-Raman-scattering efficiency and stimulated scattering in silicon," *Phys. Rev. B, Condens. Matter*, vol. 2, no. 6, pp. 1858–1862, Sep. 1970.

[89] P. A. Temple and C. E. Hathaway, "Multiphonon Raman spectrum of silicon," *Phys. Rev. B, Condens. Matter*, vol. 7, no. 8, pp. 3685–3697, Apr. 1973.

[90] D. Dimitropoulos, B. Houshmand, R. Claps, and B. Jalali, "Coupled-mode theory of Raman effect in silicon-on-insulator waveguides," *Opt. Lett.*, vol. 28, no. 20, pp. 1954–1956, Oct. 2003.

[91] T. K. Liang and H. K. Tsang, "Role of free carriers from two-photon absorption in Raman amplification in silicon-on-insulator waveguides," *Appl. Phys. Lett.*, vol. 84, no. 15, pp. 2745–2747, Apr. 2004.

[92] R. Claps, V. Raghunathan, D. Dimitropoulos, and B. Jalali, "Influence of nonlinear absorption on Raman amplification in silicon waveguides," *Opt. Express*, vol. 12, no. 12, pp. 2774–2780, Jun. 2004.

[93] M. A. Mendicino, "Comparison of properties of available SOI materials," in *Properties of Crystalline Silicon*, R. Hull, Ed. London, U.K.: Inst. Eng. Technol., 1998, ch. 18.1, pp. 992–1001.

[94] J. L. Freeouf and S. T. Liu, "Minority carrier lifetime results for SOI wafers," in *Proc. IEEE Int. SOI Conf.*, Oct. 1995, pp. 74–75.

[95] D. Dimitropoulos, R. Jhaveri, R. Claps, J. C. S. Woo, and B. Jalali, "Lifetime of photogenerated carriers in silicon-on-insulator rib waveguides," *Appl. Phys. Lett.*, vol. 86, no. 7, pp. 071115(1)–071115(3), Feb. 2005.

[96] R. Espinola, J. Dadap, R. Osgood, S. J. McNab, and Y. A. Vlasov, "Raman amplification in ultrasmall silicon-on-insulator wire waveguides," *Opt. Express*, vol. 12, no. 16, pp. 3713–3718, Aug. 2004.

[97] A. Liu, H. Rong, M. Paniccia, O. Cohen, and D. Hak, "Net optical gain in a low loss silicon-on-insulator waveguide by stimulated Raman scattering," *Opt. Express*, vol. 12, no. 18, pp. 4261–4268, Sep. 2004.

[98] S. Fathpour, O. Boyraz, D. Dimitropoulos, and B. Jalali, "Demonstration of CW Raman gain with zero electrical power dissipation in p-i-n silicon waveguides," presented at the IEEE Conf. Lasers and Electro-Optics (CLEO), Long Beach, CA, 2006, Paper CMK3.

[99] D. Dimitropoulos, S. Fathpour, and B. Jalali, "Intensity dependence of the carrier lifetime in silicon Raman lasers and amplifiers," *Appl. Phys. Lett.*, vol. 87, no. 26, pp. 261108(1)–261108(3), Dec. 2005.

[100] M. Krauss, H. Renner, E. Brinkmeyer, S. Fathpour, D. Dimitropoulos, V. Raghunathan, and B. Jalali, "Efficient Raman amplification in cladding-pumped silicon waveguides," in *Proc. Group IV Photonics Conf.*, Ottawa, ON, Canada, Sep. 13–15, 2006, pp. 61–63.

[101] F. J. Grawert, J. T. Gopinath, F. Ö. Ilday, H. M. Shen, E. P. Ippen, F. X. Kärtner, S. Akiyama, J. Liu, K. Wada, and L. C. Kimerling, "220-fs erbium–ytterbium: Glass laser mode locked by a broadband low-loss silicon/germanium saturable absorber," *Opt. Lett.*, vol. 30, no. 3, p. 329, Feb. 2005.

[102] R. Claps, V. Raghunathan, D. Dimitropoulos, and B. Jalali, "Anti-Stokes Raman conversion in silicon waveguides," *Opt. Express*, vol. 11, no. 22, pp. 2862–2872, Nov. 2003.

[103] V. Raghunathan, R. Claps, D. Dimitropoulos, and B. Jalali, "Wavelength conversion in silicon using Raman induced four-wave mixing," *Appl. Phys. Lett.*, vol. 85, no. 1, pp. 34–36, Jul. 2004.

[104] ——, "Parametric Raman wavelength conversion in scaled silicon waveguides," *J. Lightw. Technol.*, vol. 23, no. 6, pp. 2094–2102, Jun. 2005.

[105] H. Fukuda, K. Yamada, T. Shoji, M. Takahashi, T. Tsuchizawa, T. Watanabe, J. Takahashi, and S. Itabashi, "Four-wave mixing in silicon wire waveguides," *Opt. Express*, vol. 13, no. 12, pp. 4629–4637, Jun. 2005.

[106] R. Espinola, J. Dadap, R. Osgood, Jr., S. McNab, and Y. Vlasov, "C-band wavelength conversion in silicon photonic wire waveguides," *Opt. Express*, vol. 13, no. 11, pp. 4341–4349, May 2005.

[107] M. A. Foster, A. C. Turner, J. E. Sharping, B. S. Schmidt, M. Lipson, and A. L. Gaeta, "Broad-band optical parametric gain on a silicon photonic chip," *Nature*, vol. 441, no. 7096, pp. 960–963, Jun. 2006.

[108] L. R. Nunes, T. K. Liang, H. K. Tsang, M. Tsuchiya, D. Van Thourhout, P. Dumon, and R. Baets, "Ultrafast non-inverting wavelength conversion by cross-absorption modulation in silicon wire waveguides," in *Proc. 2nd IEEE Int. Conf. Group IV Photon.*, Sep. 2005, pp. 154–156.

[109] V. Raghunathan and B. Jalali, "Stress-induced phase matching in silicon waveguides," presented at the Conf. Lasers and Electro-Optics (CLEO), Long Beach, CA, May 2006, Paper CMK5.

[110] O. Boyraz, T. Indukuri, and B. Jalali, "Self-phase modulation-induced spectral broadening in silicon waveguides," *Opt. Express*, vol. 12, no. 5, pp. 829–834, Mar. 2004.

[111] O. Boyraz, P. Koonath, V. Raghunathan, and B. Jalali, "All optical switching and continuum generation in silicon waveguides," *Opt. Express*, vol. 12, no. 17, pp. 4094–4102, Aug. 2004.

[112] O. Boyraz, J. Kim, M. N. Islam, F. Coppinger, and B. Jalali, "10 Gb/s multiple wavelength, coherent short pulse source based on spectral carving of supercontinuum generated in fibers," *J. Lightw. Technol.*, vol. 18, no. 12, pp. 2167–2175, Dec. 2000.

[113] E. Dulkeith, Y. Vlasov, F. Xia, X. Chen, N. Panoiu, and R. Osgood, "Efficient self-phase-modulation in submicron silicon-on-insulator waveguides," in *Proc. CLEO*, Long Beach, CA, May 2006, Paper QTuC7.

[114] T. Indukuri, P. Koonath, and B. Jalali, "Monolithic vertical integration of metal-oxide-semiconductor transistor with subterranean photonics in silicon," in *Proc. OFC*, Anaheim, CA, Mar. 2006.

[115] J. Halloy, "Research highlights: Photonics: Silicon goes underground," *Nature*, vol. 440, no. 7085, p. 718, Apr. 2006.

[116] Courtesy of E. Pop, Stanford Univ., Stanford, CA, personal communication.

[117] D. J. Frank, "Power-constrained CMOS scaling limits," *IBM J. Res. Develop.*, vol. 46, no. 2/3, pp. 235–244, Mar.–May 2002.

[118] *International Technology Roadmap for Semiconductors*. [Online]. Available: http://www.itrs.net/

[119] O. Qasaimeh, P. Bhattacharya, and E. T. Croke, "SiGe–Si quantum-well electroabsorption modulators," *IEEE Photon. Technol. Lett.*, vol. 10, no. 6, pp. 807–809, Jun. 1998.

[120] Y. Kuo, Y. K. Lee, Y. Ge, S. Ren, J. E. Roth, T. I. Kamins, D. A. B. Miller, and J. S. Harris, "Strong quantum-confined Stark effect in germanium quantum-well structures on silicon," *Nature*, vol. 437, no. 7063, pp. 1334–1336, Oct. 2005.

[121] S. Fathpour, K. K. Tsia, and B. Jalali, "Energy harvesting in silicon Raman amplifiers," *Appl. Phys. Lett.*, vol. 89, no. 6, p. 061109, Aug. 2006.

[122] ——, "Photovoltaic effect in silicon Raman amplifiers," presented at the Optical Amplifiers and Their Applications (OAA), Whistler, BC, Canada, 2006, Paper PD1.

[123] Y. Liu and H. K. Tsang, "Raman gain in helium ion implanted silicon waveguides," in *Proc. CLEO*, Long Beach, CA, May 2006, Paper CTuU6.

[124] V. Raghunathan, R. Shori, O. Stafsudd, and B. Jalali, "Nonlinear absorption in silicon and the prospects of mid-infrared silicon Raman lasers," *J. Phys. Status Solidi, A*, vol. 203, no. 5, pp. R38–R40, Mar. 2006.

[125] M. C. M. Lee and M. C. Wu, "Thermal annealing in hydrogen for 3-D profile transformation on silicon-on-insulator and sidewall roughness reduction," *J. Microelectromech. Syst.*, vol. 15, no. 2, pp. 338–343, Apr. 2006.

[126] M. Borselli, T. J. Johnson, and O. Painter, "Beyond the Rayleigh scattering limit in high-Q silicon microdisks: Theory and experiment," *Opt. Express*, vol. 13, no. 5, pp. 1515–1530, Mar. 2005.

[127] D. Leong, M. Harry, K. J. Reeson, and K. P. Homewood, "A silicon/iron-disilicide light-emitting diode operating at a wavelength of 1.5 μm," *Nature*, vol. 387, no. 6634, pp. 686–688, Jun. 1997.

[128] W. L. Ng, M. A. Lourenço, R. M. Gwilliam, S. Ledain, G. Shao, and K. P. Homewood, "An efficient room-temperature silicon-based light-emitting diode," *Nature*, vol. 410, no. 6825, pp. 192–194, Mar. 2001.

[129] M. A. Green, J. Zhao, A. Wang, P. J. Reece, and M. Gal, "Efficient silicon light-emitting diodes," *Nature*, vol. 412, no. 6849, pp. 805–808, Aug. 2001.

[130] S. Noda and T. Asano, "SOI-based photonic crystals," in *Proc. Group IV Photon. Conf.*, Sep. 2005, pp. 27–29.

[131] S. Y. Lin, V. M. Hietala, L. Wang, and E. D. Jones, "Highly dispersive photonic band-gap prism," *Opt. Lett.*, vol. 21, no. 21, pp. 1771–1773, Nov. 1996.
[132] H. Hosaka, T. Kawashima, A. Tomita, M. Notomi, T. Tamamura, T. Sato, and S. Kawakami, "Superprism phenomena in photonic crystals," *Phys. Rev. B, Condens. Matter*, vol. 58, no. 16, pp. R10096–R10099, Oct. 1998.
[133] P. T. Rakich, M. S. Dahlem, S. Tandon, M. Ibanescu, M. Soljaci, G. S. Petrich, J. D. Joannopoplus, L. A. Kolodziejski, E. P. Ippen, "Achieving centimetre-scale supercollimation in a large-area two-dimensional photonic crystal," *Nat. Mater.*, vol. 5, no. 2, pp. 93–96, Feb. 2006
[134] M. Loncar, D. Nedeljkovic, T. Doll, J. Vuckovic, A. Scherer, and T. P. Pearsall, "Waveguiding in planar photonic crystals," *Appl. Phys. Lett.*, vol. 77, no. 13, pp. 1937–1939, Sep. 2000.
[135] M. Soljacic, S. G. Johnson, S. Fan, M. Ibanescu, E. Ippen, and J. D. Joannopoulos, "Photonic-crystal slow-light enhancement of nonlinear phase sensitivity," *J. Opt. Soc. Amer. B, Opt. Phys.*, vol. 19, no. 9, pp. 2052–2059, Sep. 2002.

Bahram Jalali (S'86–M'89–SM'97–F'04) received the B.S. degree in physics from Florida State University, Tallahassee, in 1984 and the M.S. and Ph.D. degrees in applied physics from Columbia University, New York, NY, in 1986 and 1989, respectively.

He is a Professor of electrical engineering and the Director of the Optoelectronic Circuits and System Laboratory, University of California, Los Angeles (UCLA). From 1988 to 1992, he was a Member of Technical Staff with the Physics Research Division, AT&T Bell Laboratories, Murray Hill, NJ, where he conducted research on ultrafast electronics and optoelectronics. While on leave from UCLA from 1999 to 2001, he founded Cognet Microsystems, a Los Angeles-based fiber-optic component company, where he served as the CEO, President, and Chairman from the company's inception through its acquisition by Intel Corporation in April 2001. From 2001 to 2004, he served as a Consultant with Intel Corporation. He has published more than 200 scientific papers. He is the holder of six U.S. patents. His current research interests are in silicon photonics and ultrafast photonic signal processing.

Dr. Jalali is a Fellow of the Optical Society of America, the Chair of the Los Angeles Chapter of the IEEE Lasers and Electro-Optics Society, and a Member of the California NanoSystems Institute. He serves on the Board of Trustees of the California Science Center. He was chosen by the *Scientific American Magazine* as one of the 50 Leaders Shaping the Future of Technology in 2005. He has received the BridgeGate 20 Award for his contribution to the southern California economy.

Sasan Fathpour (S'01–M'04) received the B.S. degree from Isfahan University of Technology, Isfahan, Iran, in 1995, the M.A.Sc. degree from the University of British Columbia (UBC), Vancouver, BC, Canada, in 2000, and the Ph.D. degree from the University of Michigan, Ann Arbor, in 2005, all in electrical engineering. His research at UBC was on nitride heterojunction bipolar transistors. His Ph.D. research was on epitaxial growth, fabrication, characterization, and modeling of In(Ga)As self-assembled quantum dot lasers, with record-high dynamic and static performances, as well as on spin-polarized light sources based on diluted magnetic III–V semiconductors.

From 1995 to 1997, he was with Isfahan Optical Industry and was engaged in the research and development of microelectronic circuits and DSP systems with Pardisan Inc. in 1998. He is currently a Postdoctoral Research Fellow with the University of California, Los Angeles, researching silicon photonics, particularly applications of nonlinear optical effects in active silicon optoelectronic devices. He is the coauthor of about 50 journal and conference publications.